2018

REGULATION OF UBIQUITIN SPECIFIC PEPTIDASE 2 EXPRESSION BY FARNESOID X RECEPTOR IN HEPATOCELLULAR CARCINOMA

Christina Nadolny
University of Rhode Island, cnadolny@my.uri.edu

REGULATION OF UBIQUITIN SPECIFIC PEPTIDASE 2 EXPRESSION BY FARNESOID X RECEPTOR IN HEPATOCELLULAR CARCINOMA

BY

CHRISTINA NADOLNY

A DISSERTATION SUBMITTED IN PARTIAL FULFILLMENT OF THE

REQUIREMENTS FOR THE DEGREE OF DOCTOR OF PHILOSOPHY

IN

BIOMEDICAL AND PHARMACEUTICAL SCIENCES

UNIVERSITY OF RHODE ISLAND

2018

DOCTOR OF PHILOSOPHY DISSERTATION

OF

CHRISTINA NADOLNY

APPROVED:

Dissertation Committee:

Major Professor: Ruitang Deng

David A. Rodrigues

Gongqin Sun

Nasser H. Zawia

DEAN OF THE GRADUATE SCHOOL

UNIVERSITY OF RHODE ISLAND

2018

ABSTRACT

Liver cancer is in the ten leading cancer types for estimated new cases and deaths in the United States in 2018, and is often detected at late stages when it is rapidly fatal. Of the types of liver cancers in humans, hepatocellular carcinoma (HCC) is the most lethal and prevalent. An important factor in the development of HCC is Farnesoid X Receptor (FXR). FXR acts as master regulator of bile acid homeostasis, and is involved in lipid, cholesterol, and glucose homeostasis. In addition, it plays a protective role against HCC, the precise mechanisms of which has yet to be identified.

Ubiquitin Specific Peptidase 2 (USP2) has emerged as a promising area of research for cancer therapy for multiple organ systems. Recent studies have shown USP2 to be involved in a variety of cellular processes ranging from circadian rhythms to tumorigenesis. In particular, USP2 has been studied in lung, bladder, breast, prostate, and ovarian cancer. Additionally, USP2 has 3 distinct isoforms, USP2a, USP2b, and USP2c, all of which have unique functions. In manuscript 1, the purpose of the study was to investigate the isoform specific effects of USP2 in hepatocellular carcinoma (HCC) through the use of healthy human liver samples compared to tumor samples, paired human liver tumor and surrounding samples, paired mouse liver tumor and surrounding samples, and the immortalized liver cancer cell line HepG2. Of the three USP2 isoforms, USP2a and USP2b are the most abundant in human and murine liver. Both USP2a and USP2b levels are significantly lower in HCC compared to healthy liver samples. In paired tumor and surrounding liver samples from mice and human, USP2b is consistently decreased within the tumor compared to the surrounding tissue. USP2b was decreased in tumors in all human samples and decreased in over 80% of murine

samples. This suggests as the state of the liver worsens in HCC pathology, USP2b will also decrease. In HepG2 cells, both USP2a and USP2b isoforms led to increased proliferation, colony formation, and wound healing. Additionally, USP2b and USP2c lead to increased migration, wound healing, and apoptosis. Previous studies have only recognized USP2b as a circadian gene, making this the first study to report involvement of USP2b in cellular processes beyond its circadian characteristics. Overall, USP2a and USP2b have opposing roles in HCC development, with USP2a displaying a tumor-promotion role and USP2b displaying a tumor-protective role.

In manuscript 2, we present a novel potential mechanism for USP2 regulation in the liver and in HCC development through FXR. Between wild type and FXR-/- mice, there was a dysregulation in USP2 and previously identified downstream targets. To determine if the changes in USP2 were due to FXR regulation, we activated FXR in wild type mice, over-expressed FXR in liver cancer cells, and evaluated the effects of FXR activation on the USP2 promoter. Upon treatment with FXR agonist in wild type mice, USP2 mRNA and protein significantly increased compared to vehicle. Additionally, transfection and activation of FXR in huh7 cells lead to an increase in USP2. Of importance, we found FXR directly regulates USP2 gene expression via dual luciferase assay. This study is the first to report FXR in the regulation of gene, mRNA, and protein expression of USP2 in the liver. Specifically, FXRα2 is the predominant isoform in this regulation. In addition, this is also the first study to identify the different USP2 isoforms to be a results of two promoters rather than alternative splicing. As previous studies have found FXR to display a protective effect in HCC, this study identifies a novel mechanism of this protection through USP2.

ACKNOWLEDGEMENTS

I would like to thank my major professor Dr. Ruitang Deng for his guidance over my graduate school career. Not only was he a great mentor, but also a wonderful teacher and role model. Dr. Deng has allowed me to grow as a student through his encouragement of a deeper understanding of the scientific process and independent thought. I now feel confident in my abilities as a scientist and a leader, both of which I owe to Dr. Deng.

I would like to thank my committee members, Dr. David Rodrigues, Dr. Gongqin Sun, and Dr. Joel Chandlee, for offering their time, encouragement, and input into my research. Throughout their time on my committee, they have offered valuable insight into my project and were always happy to help.

I am thankful to the American Foundation for Pharmaceutical Education (AFPE) for granting me a Pre-Doctoral Fellowship for two years. This allowed me to fully focus on my research and successfully complete my degree.

I am grateful for my friends and family who have supported me throughout my graduate school career, even when things seemed stressful or unattainable. Their continued encouragement and unwavering love has been vital to the completion of my degree.

PREFACE

This dissertation was prepared following manuscript format. It is divided into two manuscripts focusing on Ubiquitin Specific Peptidase 2 (USP2). The first manuscript centers on the three USP2 isoforms, USP2a, USP2b, and USP2c. The isoform dependent relationship is explored in hepatocellular carcinoma (HCC) through the utilization of human HCC samples, mice tumor samples, and immortalized HCC cells. The second manuscript investigates how USP2 is regulated by Farnesoid X Receptor (FXR) in HCC. This manuscript is the first to suggest FXR as a novel regulator of USP2, and is also the first to identify two promoters as the source for the different USP2 isoforms. Both manuscripts have been prepared for submission in Hepatology.

TABLE OF CONTENTS

Page

LIST OF FIGURES

FIGURE PAGE

Manuscript 1

Manuscript 2

LIST OF TABLES

TABLE PAGE

Manuscript 1

MANUSCRIPT – I

Characterization of Oncogenic Effects of Ubiquitin Specific Peptidase 2 Isoforms in Hepatocellular Carcinoma

Christina Nadolny, Yuan Chen, and Ruitang Deng

(Prepared for submission Hepatology)

Isoform Specific Effects of Ubiquitin Specific Peptidase 2 in Hepatocellular Carcinoma Development

Christina Nadolny, Yuan Chen, and Ruitang Deng

Department of Biomedical and Pharmaceutical Sciences, Center for Pharmacogenomics and Molecular Therapy, College of Pharmacy, University of Rhode Island, 7 Greenhouse Road, Kingston, RI 02881

Christina Nadolny: cnadolny@my.uri.edu

Yuan Chen: chenyuan@uri.edu

Ruitang Deng: dengr@uri.edu

Key Words: USP2, HCC, Liver, Deubiquitin, Ubiquitin

FOOTNOTES

Contact Information:

Ruitang Deng**,** Department of Biomedical and Pharmaceutical Sciences, Center for Pharmacogenomics and Molecular Therapy, College of Pharmacy, University of Rhode Island, Kingston, RI 02881. Tel: 401-874-4950. Fax: 401-874-5787. Email: DengR@uri.edu.

Abbreviations:

USP2: Ubiquitin Specific Peptidase 2

HCC: Hepatocellular Carcinoma

MDM2: Murine Double Minute 2

NPAS: Neuronal PAS Domain Protein 2

ARNTL: Aryl Hydrocarbon Receptor Nuclear Translocator-Like

BMAL: Brain and Muscle Arnt-Like

PER: Period

CRY: Cryptochrome

RIP: Receptor-Interacting Serine/Threonine Protein kinase

MEM: Minimum Essential Media

FBS: Fetal Bovine Serum

NEAA: Non-Essential Amino Acids

RLU: Relative Luminescence Units

RFU: Relative Fluorescence Units

ECM: Extracellular Matrix

HCC-T: HCC tumor

HCC-NT: HCC non-tumor

CHTN: Cooperative Human Tissue Network

PCR: Polymerase Chain Reaction

GAPDH: Glyceraldehyde-3-phosphate dehydrogenase

PMSF: Phenylmethylsulfonyl Fluoride

PVDF: Polyvinylidene Difluoride

pTNM: Pathologic Tumor-Node-Metastasis

FXR: Farnesoid X Receptor

Financial Support:

This work was supported by the National Institutes of Health Grants R01DK087755 and R01CA213419. Additional support for CN was provided by the American Foundation for Pharmaceutical Education (AFPE) Pre-Doctoral Award in Pharmaceutical Sciences.

ABSTRACT

Ubiquitin Specific Peptidase 2 (USP2), a deubiquitinating enzyme, has been shown in recent research to be involved in a variety of cellular processes ranging from circadian rhythms to tumorigenesis. In particular, USP2 has been studied in lung, bladder, breast, prostate, and ovarian cancer. The purpose of this study was to investigate the isoform specific effects of USP2 in hepatocellular carcinoma (HCC) through the use of healthy human liver samples compared to tumor samples, paired human liver tumor and surrounding samples, paired mouse liver tumor and surrounding samples, and the immortalized liver cancer cell line HepG2. Of the three USP2 isoforms, USP2a and USP2b are the most abundant in human and murine liver. Both USP2a and USP2b levels are significantly lower in HCC compared to healthy liver samples. Additionally, we see a trend of decreasing USP2b from normal healthy liver, to surrounding tissue, to tumor tissue in humans. In paired tumor and surrounding liver samples from mice and human, USP2b is consistently decreased within the tumor compared to the surrounding tissue. USP2b was decreased in tumors in all human samples and decreased in over 80% of murine samples. This suggests as the state of the liver worsens in HCC pathology, USP2b will also decrease. In HepG2 cells, both USP2a and USP2b isoforms led to increased proliferation, colony formation, and wound healing. Additionally, USP2b and USP2c lead to increased migration, wound healing, and apoptosis. Previous studies have only recognized USP2b as a circadian gene, making this the first study to report involvement of USP2b in cellular processes beyond its circadian characteristics. Overall, USP2a and USP2b have opposing roles in HCC

development, with USP2a displaying a tumor-promotion role and USP2b displaying a tumor-protective role.

INTRODUCTION

The control of protein turnover is a fundamental aspect of cellular processes. Of importance in maintenance of proper protein levels is rate of synthesis and rate of degradation. The two major pathways that mediate protein degradation are the ubiquitin-proteasome system and lysosomal proteolysis. Of the two, the ubiquitin-proteasome system is the major pathway for selective protein degradation in eukaryotic cells (1). Ubiquitin can bind to its substrate and signal for protein degradation, altered cellular location, as well as promotion or prevention of protein interaction (2). Ubiquitination can be reversed by deubiquitinating enzymes, such as Ubiquitin Specific Peptidase 2 (USP2). USP2 has emerged as a promising area of research for cancer therapy for multiple organ systems. However, it is important to note that USP2 has multiple isoforms due to alternative splicing of 5' exons (3), all of which have different actions and expression levels within cells. USP2a (NM_004205), also known as variant 1 or USP2-69, encodes the longest isoform with 619 amino acids. USP2b (NM_171997), also known as variant 2 or USP2-45, is a shorter isoform comprised of 396 amino acids and a different N-terminus. USP2b is missing 2 exons from the 5' end and contains an alternative 5' terminal exon compared to transcript variant 1. USP2c (NM_001243759), also known as variant 3 or USP2-41, is missing internal exon 2 in the 5' region. USP2c is the shortest of the isoforms with 362 amino acids.

USP2a has been reported in a variety of tumorigenic studies. USP2a expression enhances proliferation, invasion, and migration in bladder cancer by stabilizing cyclin A1 (4), plays a critical role in prostate cancer cell survival through fatty acid synthase stabilization (5), and has shown aberrant expression in breast (6), lung (7), and ovarian

cancer (8). Additionally, multiple studies report USP2a to be involved in the regulation of Myc and p53. Myc is a proto-oncogene which is overexpressed in many types of human cancer, and p53 is a well-known tumor suppressor negatively regulated by Mdm2 and Mdmx (9). USP2a was found to regulate the p53 pathway by selectively targeting Mdm2 in cells (10), and was found to form a complex with MdmX both *in vitro* and *in vivo* and regulate its stability (11). Furthermore, USP2a targets c-Myc via the miRNA cluster miR-34b/c by directly impairing the MDM2-p53 pathway in prostate cancer (12).

USP2b is the isoform most noted for its circadian patterns. When USP2 was first identified as a highly rhythmic circadian gene in multiple tissues, the various isoforms were not separated (13,14). Upon further investigation of the isoforms, literature suggests a potential role for both USP2a and USP2b in circadian rhythms. Core clock components include CLOCK, NPAS, ARNTL/BMAL1, PER, and CRY (15). The USP2b isoform was reported to complex with clock components as well as stabilize BMAL1, which then alters expression of several CLOCK/BMAL1 regulated genes (16). In addition, both USP2a and USP2b were shown to interact directly with PER via co-immunoprecipitation and reciprocal immunoprecipitation. However, this deubiquitination does not affect its overall stability (17). Interestingly, USP2a was found to deubiquitinate and stabilize CRY1 protein in both cell culture and mouse liver, an effect that was not seen with USP2b. When USP2 is depleted, ubiquitination of CRY1 enhances and dampens oscillation amplitude of CRY1 protein during a circadian cycle (18). In the current study, mRNA expression in mouse liver samples show a dramatic circadian pattern of USP2b, with minimal circadian rhythm of USP2a. For all

experiments, total USP2 followed the same pattern as USP2b and overshadowed the USP2a isoforms for TaqMan qPCR, which is why all are reported as USP2a and USP2b.

Finally, little has been reported regarding USP2c. Conflicting reports claim no evidence supporting its existence (3), while others reported isolation of USP2c in a screen for proapoptotic genes (19). The later report found USP2c to elicit all features of apoptosis in human cells. This same research group found both USP2a and USP2c to cause apoptosis in MCF7 cells by targeting receptor-interacting serine/threonine protein kinase 1 (RIP1) (20).

Here, we investigated the tumor-promotion or protective effects of the 3 USP2 isoforms in healthy human liver samples compared to tumor samples, paired human liver tumor and surrounding samples, paired mouse liver tumor and surrounding samples, and the immortalized liver cancer cell line HepG2. Compared to healthy human liver samples, both USP2a and USP2b have statistically significant reductions compared to HCC patients. When comparing 8 paired HCC samples separated into tumor versus surrounding tissue, USP2a is increased in 4 tumor samples while decreased in the other 4 tumor samples. Of these same samples, USP2b was decreased in all tumor samples, with an average of an 82% reduction. Of 26 paired mouse tumor versus surrounding tissue samples, 14 had increased USP2a within the tumor section. Of these same samples, 22 of the 26 samples had decrease USP2b within the tumor section, with 19 samples showing a greater than 20% reduction and 13 samples having greater than a 50% reduction. In HepG2 cells, both USP2a and USP2b increased cell proliferation, wound healing, and colony formation properties. USP2b and USP2c, but not USP2a, showed increased apoptosis in, and no isoforms showed necrotic properties.

Overall, consistent with previous literature USP2a shows dysregulation between normal and HCC samples. However, USP2b also displays dramatic changes in human and mouse tumor samples. Taken together, with a decrease in paired tumor versus surrounding samples in both humans and mice, as well as decreased levels in normal compared to HCC patients, USP2b correlates with a healthy phenotype and decreases as the state of the liver worsens. This is the first report of the USP2b isoform being involved in tumor formation, as opposed to the common focus in circadian patterns.

MATERIALS AND METHODS

Cell Culture: Immortalized HCC HepG2 cells (ATCC, cat# HB-8065) were utilized for all cell culture assays. Cells were cultured in Minimum Essential Media (MEM) (Thermo Fisher Scientific, cat# 11095080) complete media containing 10% Fetal Bovine Serum (FBS) (Atlanta biologicals, cat #S11550), 1% PenStrep (Thermo Fisher, cat# 15140122), and 1% Non-Essential Amino Acids (NEAA) (Thermo Fisher, cat# 11140050). For those assays requiring serum starving, MEM contained 1% FBS, 1% PenStrep, and 1% NEAA. Cells were cultured at 37^{o}C in a humidified atmosphere containing 5% CO_2.

Transfection: GenJet Reagent (Version II) (SignaGen, cat# SL100489) was used for transfection of USP2 plasmid constructs. Cells were seeded at 80% density prior to transfection. Cells were transfected for 16 hours then media was replaced with complete serum/antibiotic media.

Plasmid Constructs: Plasmids used for transfection include human USP2a, USP2b, and USP2c. All plasmids are in pcDNA3.1(+) vector with HindIII-BamHI cloning sites. USP2a is 1839bp, USP2b is 1212bp, and USP2c is 1110bp and are codon optimized to enhance the expression in human cell lines. Sequences are detailed in supplement table 1.

Colony Formation: USP2 isoform specific transfected cells were seeded at a low density of 600 cells per well in a 6 well plate and allowed to grow for 7 days. Complete media was changed every 2 days. Cells were fixed using 1:7 acetic acid to methanol solution and stained with crystal violet. Colonies were quantified using ImageJ cell counter plug in.

Proliferation Assay: Cells were seeded at 70% confluence and transfected with USP2a or USP2b for 24 and 48hrs. After each time point, trypsin was added and cells were counted using a haemocytometer. For each well, cells were counted in the 4 sets of 16 corner squares and an average was taken. The final average was taken of the set run in triplicate.

Apoptosis and Necrosis assay: Cells were seeded at 70% confluence and transfected with USP2a, USP2b, and USP2c. RealTime-Glo Annexin V Apoptosis and Necrosis Assay (Promega, cat# JA1011) was used to distinguish between healthy cells and those in early apoptosis or secondary necrosis. Detection reagent was added to complete media and incubated for 0, 6, 12, and 24, and 48 hours. Relative luminescence units

(RLU) and relative fluorescence units (RFU) were measured using a GloMax Multimode Microplate Reader (Promega) with green spectrum fluorescence ($485nm_{Ex}$/$525–530nm_{Em}$).

Wound Healing Assay: Cells were seeded in a 6 well plate in serum starved media and transfected with codon optimized USP2 plasmids for 16 hours. Cells were counted and seeded in triplicate into CytoSelect 24-Well Wound Healing Assay plates (Cell Biolabs Inc, cat # CBA-120). Inserts create a wound field with a defined gap of 0.9 mm. Cells were allowed to adhere overnight for a monolayer to form. Inserts were carefully removed from each well using sterile forceps. Media was removed and the wounded monolayer was washed with sterile PBS twice before addition of serum starved media. Photographs were taken using EVOS Cell Imagining Microscope (ThermoFisher Scientific) at time 0 when wound was created, as well as 24 and 48 hours post insert removal. Average percent wound closure was calculated using ImageJ based upon 3 random fields per well. Student t-test was then used to determine significance of percent wound closure compared to control.

Cell Migration Assay: Cells were seeded in a 6 well plate in serum starved media and transfected with codon optimized USP2 plasmids for 16 hours. Cells were counted and seeded in triplicate into CHEMICON QCM Migration Assay (Millipore Sigma, cat# ECM508), which is based upon the Boyden Chamber principle. The top chamber of the plate had an 8μm pore size polycarbonate membrane. The bottom chamber contained 10% FBS media as a chemoattractant. Following incubation for 48 hours, cells which

migrated through the insert membrane were stained for 20 minutes at room temperature. Inserts were then dipped in water to rinse. Cells on the interior of the insert were mechanically removed. The stain was then extracted and transferred for colorimetric measurement at 560 nm using a GloMax Multimode Microplate Reader (Promega).

Invasion Assay: CHEMICON Cell Invasion Assay Kit (Millipore Sigma, cat# ECM550) was utilized for observation of invasive properties. The same steps were followed for seeding, transfecting, and quantification as described in the cell migration assay section above. However, this kit also includes an extracellular matrix (ECM) layer in the insert. For cells to migrate through the 8μm pore, they must be able to first pass through this ECM layer, indicating increased invasive properties.

Human Liver samples: Twelve healthy human liver samples and 18 HCC tumor (HCC-T) samples with 8 paired adjacent non-tumor (HCC-NT) tissues were obtained from the University of Virginia, University of Pennsylvania and Ohio State University through the Cooperative Human Tissue Network (CHTN). The detailed information on HCC patients is provided in Supplement Tables 2 and 3. The protocol for using human tissues was approved by the Institutional Review Board (IRB) at the University of Rhode Island (URI).

Animal Experimentation: All animals received humane care according to the criteria outlined in the "Guide for the Care and Use of Laboratory Animals" prepared by the National Academy of Sciences and published by the National Institutes of Health (NIH

publication 86023 revised 1985). In total, 26 $FXR^{-/-}$ mice between the ages of 14-18 months were utilized. Of these mice, 12 were female and 14 were male. Mice were fed a regular chow diet and housed in Innovive IVC ventilated rodent housing system racks in IVC disposable cages. Since $FXR^{-/-}$ mice will spontaneously develop liver tumors as they age without additional insult, all 26 mice had liver tumor formation. Paired surrounding and tumor tissue sections were collected separately for comparison. All samples were snap frozen in liquid nitrogen.

Quantitative real-time PCR: Total RNA was prepared from human liver samples and $FXR^{-/-}$ mouse samples by phenol-chloroform extraction using RNA-Bee RNA isolation reagent (Amsbio, cat #CS-501B) according to the manufacturer's protocol. RNA was quantified by measuring its absorbance at 280 nm in a UV-visible spectrophotometer (NanoDrop ND 1000; Thermo Fisher Scientific). M-MLV Reverse Transcriptase (Promega, cat #M170B) was utilized to synthesize cDNA. TaqMan Gene Expression Assay was utilized for analysis of cDNA. All TaqMan probes were purchased through Thermo Fisher Scientific and are as follows. Human total USP2 (cat# Hs00275859_m1), USP2a (cat# Hs00374431_m1), and USP2b (Hs01592505_m1) were purchased from catalog. Mouse total USP2 (cat# Mm00497452_m1) and USP2b (cat# Mm01168648) probes were purchased from catalog. The Custom TaqMan Assay Design Tool (cat# 4441114) was utilized for custom design of mouse USP2a probe based on NM_016808 (Assay ID ARCE37A). Applied Biosystems ViiA 7 Real-Time PCR instrument was used for quantification using the comparative C_T ($\Delta\Delta C_T$) method

normalized against glyceraldehyde-3-phosphate dehydrogenase (GAPDH) housekeeper.

Western Blotting: Liver tissue was homogenized in sucrose-Tris (ST) buffer composed of 0.25 M sucrose and 10 mM Tris-HCL with ph 7.4 containing Halt Protease Inhibitor Cocktail (Thermo Scientific, cat #87785) and phenylmethylsulfonyl fluoride (PMSF) (Sigma, CAS #329986). Membrane fractions containing total proteins were loaded into each well. After overnight wet transfer to polyvinylidene difluoride (PVDF) membrane, the membrane was probed for the various USP2 isoforms. Sequence specific antibodies were purchased from Biomatik, and are detailed in supplementary table 3. Additionally, the following antibodies were purchased: Cycin D1 (Santa Cruz cat# sc-8396), FAS (Santa Cruz cat# sc-55580), MDM2 (Santa Cruz cat# sc-965), P53 (Santa Cruz, cat #sc-47698), and USP2 (SantaCruz cat #sc-135282). Rabbit anti-human GAPDH polyclonal antibody (Sigma-Aldrich, cat# G9545) was used a as housekeeper to normalize protein expression. Based upon the primary antibody, goat-anti rabbit or goat-anti mouse IgG HRP was used for secondary antibody incubation. Clarity and Clarity Max Western ECL Blotting Substrates (BioRad cat# 1705060) was added to membranes for chemiluminescent detection, incubated according to protocol, and imaged using myECL Imager from Thermo Scientific. ImageJ was used to quantify bands.

Statistical analysis: Student t-test was applied to pair-wise comparison for normally distributed data. Non-parametric Mann-Whitney test was used for pair-wise comparison

for non-normally distributed data. P value of 0.05 or lower was considered statistically significant.

RESULTS

USP2a is decreased in HCC patients.

USP2a has been implicated in development of other cancers (4–8). To determine whether USP2a plays any roles in HCC development, hepatic expression levels of USP2a in healthy and HCC subjects were quantified. A total of 12 normal samples, 8 paired HCC-NT (surrounding non-tumor) and HCC-T (tumor), and an additional 10 HCC tumor samples (not paired) were compared.

Hepatic USP2a mRNA levels are significantly decreased in HCC patient samples compared to normal liver tissue samples. Compared to healthy, there is a statistically significant decrease in all sample groups, with an 80%, 55%, 79%, 69% decrease in the HCC-NT (paired), HCC-T (paired), HCC (non-paired), and HCC-T (combined), respectively (fig 1a). The results demonstrated that hepatic USP2a expression was significantly deceased in HCC subjects when compared to normal subjects. Interestingly, these results are contradictory to a published study where they found increased levels of USP2a in HCC samples compared to normal subjects (21). This is addressed in the discussion section.

USP2a is dysregulated in human tumor compared to surrounding tissue.

A decrease is seen in USP2a expression levels in HCC tumor samples compared to normal liver samples. To determine whether USP2a is also dysregulated once HCC

has already developed, hepatic expression levels of USP2a in paired surrounding and tumor samples were quantified. There was an interesting relationship of USP2a between paired surrounding and tumor samples from a single patient. Taken as an average, there is a 3.12 fold increase in USP2a in tumor samples (fig 1b). However, when comparing each sample as a pair, half of them show over a 3 fold increase, and the other half show over a 65% decrease (fig. 1c). The characteristics of the subjects is summarized in supplement table 2. There seems to be no trend between USP2a levels for gender, race, age, histologic grade, pathological tumor-node metastasis (pTNM), focality, or tumor size, indicating another factor may have a role in regulating USP2a in HCC. These results demonstrate a more complex role of USP2a expression in tumor versus surrounding tissue, suggesting an additional factor beyond tissue status regulates USP2a expression in HCC. Hypotheses for this additional factor is addressed in the discussion section.

USP2b is decreased in HCC patients.

Unlike USP2a, little is reported on USP2b in the development of other cancers. To determine if USP2b plays a role in HCC development, hepatic expression levels of USP2b in healthy and HCC subjects were quantified. Similar to USP2a, USP2b mRNA levels were also significantly decreased in HCC patient samples compared to normal liver tissue samples. A total of 12 normal samples, 8 paired HCC-NT and HCC-T, and an additional 10 HCC samples (not paired) were compared. From healthy, to HCC surrounding, to HCC tumor samples there is a steady decrease in USP2b. Compared to healthy, there is a statistically significant decrease in the tumor samples, with a 39%,

92%, and 92% decrease in the HCC-NT (paired), HCC-T (paired), and HCC-T (combined), respectively (fig 2a). Compared to USP2a, USP2b displays a more dramatic decrease in hepatic mRNA levels. Additionally relative mRNA expression of both isoforms were compared for the healthy, HCC-NT, HCC-T, and HCC (non-paired). Based upon the change in CT value, the smaller the value the more abundant the mRNA. In both healthy and HCC-NT samples, USP2b is the more abundant isoform. In HCC-T and HCC (non-paired), levels are comparable (fig. 3), suggesting USP2b may play a more important role in HCC than USP2a.

USP2b decreased in human tumor compared to surrounding tissue.

A decrease is seen in both USP2a and USP2b expression levels in HCC tumor samples compared to normal liver samples. To determine whether USP2b is also dysregulated once HCC has already developed, hepatic expression levels of USP2b in paired surrounding and tumor samples were quantified. In these same 8 paired tumor and surrounding human samples, there was a statistically significant decrease in USP2b within the tumor. Taken as an average, there is an 81% decrease in tumor samples compared to surrounding (fig 2b). When comparing each sample, all of them showed over a 50% reduction in USP2b compared to surrounding, with 5 of the 8 showing a 90% or greater reduction (fig. 2c). Likewise, there's a significant 68% reduction in USP2b protein in HCC-NT compared to their surrounding pairs (fig. 2d). Of the 8 paired samples, only 6 were available for protein analysis. Unlike USP2a, USP2b displayed a more consistent decrease in tumor sections compared to their surrounding pair, once

again suggesting USP2b is the more abundant, and may be the more influential isoform, in HCC.

USP2a is dysregulated in murine tumors compared to surrounding tissue.

In the current study, USP2a expression was decreased in HCC subjects compared to healthy subjects. Additionally, there was a dysregulation of USP2a when comparing HCC surrounding and tumor samples, half showing an increase and half showing a decrease. To determine if this same pattern is seen in murine samples, hepatic expression levels of USP2a were quantified in tumor versus surrounding tissue. Similar to the human HCC paired samples, about half of the murine samples showed increased USP2a mRNA while the other half showed a decrease. Of 26 paired mouse tumor versus surrounding tissue samples, 14 had increased USP2a within the tumor section while 12 had a decrease. Of these, 8 mice had over a 2 fold increase, while 6 had over a 50% decrease (fig. 4). Age and gender did not show any distinction in magnitude of change of USP2a. In addition, histology and grade of the tumors among the mice were comparable. These results are consistent with the human data comparing surrounding and tumor tissue. Similar to human samples, about half are increased and half are decreased, once again suggesting an additional factor beyond tissue status in the regulation of USP2a expression.

USP2b decreases in murine tumors compared to surrounding tissue.

In the current study, USP2b expression was decreased in HCC subjects compared to healthy subjects. Similarly, when comparing HCC surrounding and tumor

samples, all showed a decrease in USP2b levels. To determine if this same pattern is seen in murine samples, hepatic expression levels of USP2b were quantified in tumor versus surrounding tissue. Of the 26 paired samples, 22 samples had decrease USP2b mRNA within the tumor section, with 19 samples showing a greater than 20% reduction and 13 samples having greater than a 50% reduction (fig. 5). The four samples that had increased USP2b showed no unique identifier of age, gender, histology, or grade of the tumors. These results are consistent with human data from the current study where hepatic USP2b is decrease in HCC compared to normal human samples, and decreased in tumor compared to surrounding samples. In addition, liver samples were taken from healthy wild type mice every 4 hours for a total of 24 hours and hepatic USP2a, USP2b, and total USP2 was quantified. The total USP2 and USP2b probe displayed similar abundance, as displayed in the change in CT values, while USP2a was less abundant. Additionally, it is important to note that the total USP2 probe follows the same trend as USP2b, as this is the more abundant isoform in the mouse liver (fig. 6). Like the human liver, murine USP2b is more abundant than USP2a. With consistent USP2b data in murine samples, this again suggests USP2b may be the more important isoform in HCC.

USP2a and USP2b isoforms increase proliferation colony formation, and wound healing.

Both USP2a and USP2b were determined to be dysregulated in human HCC samples and murine tumor versus surrounding tissue. To determine if the over-expression of these isoforms would lead to functional change in hallmarks of cancer,

HepG2 cells were transfected with vector, USP2a, or USP2b, and proliferation wound healing, and colony formation were examined.

USP2a transfected cells had increased 25% and 30% compared to control after 24 and 48 hours, respectively. USP2b transfected cells had a 15% increase and 20% increase compared to control after 24 and 48 hours, respectively. For both isoforms at both time points there was a statistically significant increase in cell number (figure 7a&b). These results demonstrate when either isoform is overexpressed in HepG2 cells, cell proliferation increases.

For colony formation, cells were transfected with vector, USP2a, or USP2b for 24 hours prior to resuspension and counting. Cells were seeded at low density and allowed to grow in 10% FBS for two weeks. Both USP2a and USP2b showed a statistically significant increase in colony number compared to control. There were 28, 66, and 77.5 colonies formed in control, USP2a, and USP2b transfected cells, respectively (figure 7c). Increased colony formation properties indicate cells ability to undergo unlimited division, suggesting both isoforms increase proliferation over long term.

Similarly, HepG2 cells were transfected with vector, USP2a, or USP2b, and underwent wound healing assay. Between initial wound infliction and 48 hours post, there was a 21.33%, 32.33%, and 29.33% wound closure in control, USP2a, or USP2b, respectively. The wound closure of USP2a and USP2b compared to control was statistically significant (figure 7d). This increased wound healing with USP2 transfected cells indicate an increase in migration. As the cells were serum starved, proliferative effects should be minimized.

USP2b and USP2c increase migration, invasion, and apoptosis.

Cells were transfected with vector, USP2a, USP2b, or USP2c for 24 hours prior to counting and transfer to CHEMICON QCM Migration Assay inserts and CHEMICON Cell Invasion Assay inserts. Compared to control, there was an 8%, 15%, and 17% increase in migration of HepG2 cells across the membrane in USP2a, USP2b, and USP2c, respectively. Overall, USP2b and USP2c increased migration while USP2a showed minimal change. Of the isoforms, USP2c was the only one to show a statistically significant increase (figure 8a). Compared to control, there was a 15% increase in invasion across the extracellular matrix for both USP2b and USP2c. For USP2a, there was minimal change (figure 8b). These results demonstrate USP2b and USP2c can move from an area with confluent cells to an area with no cells when no barrier is present. The addition of the ECM adds a barrier for the cells to have to go through, indicating additional challenge for the cells. This suggests the USP2b and USP2c isoforms have more aggressive migration and invasion properties than USP2a.

In additional to proliferation, migration, and invasion, evading apoptosis is a hallmark of cancer. To examine apoptosis, cells were transfected with vector, USP2a, USP2b, or USP2c before monitoring apoptosis and necrosis using the RealTime-Glo Annexin V Apoptosis and Necrosis Assay. For 6 and 12 hours, no change was reported. After 24 hours, there was a 3.06 and 3.66 fold increase in RLU of USP2b and USP2c compared to vector, indicating apoptosis. Minimal change was seen in USP2a transfected cells, suggesting only USP2b and USP2c induce apoptosis in HepG2. For all time points, minimal change was seen between vector and any USP2 isoform for

necrosis determined by RFU (figure 8c). These results demonstrate increased apoptosis in cells overexpressing USP2b and USP2c, but not USP2a. Evading apoptosis is a hallmark of cancer, suggesting that within HepG2 cells, USP2a displays this property of cancer, while overexpressed USP2b and USP2c do not evade apoptosis. Interestingly, USP2b shows characteristics of both apoptosis and proliferation. This phenomenon is explained in the discussion section.

DISCUSSION

We have found that the 3 different USP2 isoforms have distinct characteristics that make them unique from one another. However, only USP2a and USP2b are endogenously expressed in human and mice samples at levels quantifiable by TaqMan qPCR, so they will be the focus of the discussion. Ectopic expression of USP2c was studied in the liver, however it is important to note endogenous levels are usually very low or nonexistent. Additionally, it is critical to separate USP2 by isoform in the liver. As displayed in fig. 6, the total USP2 probe displayed a significant circadian pattern, similar to that of USP2b. However, expression levels of the USP2a probe were lower and did not follow the same pattern. If specific isoforms were not separated, the data could be misinterpreted, and total USP2 would in fact reflect the changes seen in USP2b, not USP2a, as this is the more abundant isoform in the mouse liver. A previous study analyzing isoform specific expression of USP2b in a variety of tissues shows similar results in mRNA expression via northern blot. Catalytic core and USP2b probes showed similar expression, while minimal to no USP2a was seen (3).

A variety of functional assays were utilized to evaluate properties of cancer. The 6 hallmarks of cancer include evading apoptosis, self-sufficiency in growth signals, insensitivity to anti-growth signals, tissue invasion and metastasis, limitless replicative potential, and sustained angiogenesis (22). The assays utilized include proliferation, colony formation, wound healing, migration, invasion, and apoptosis. Both proliferation assay and colony formation assay assess the cells ability for sustaining proliferative signaling, with colony formation assessing long-term effects (23). Wound healing and the Boyden Chamber Migration assay assesses cell migration. The invasion assay assessed the invasive properties of the HepG2 cells. Migration is the movement of cells without having any barriers, while invasion requires cells to destroy barriers, such as ECM, in order to pass through (24). Finally, apoptosis assay assesses ability of cells to resist cell death. HepG2 cells were utilized for functional assays since they show very low expression of USP2b and USP2c. Huh7 cells, another HCC cell line, expressed both USP2a and USP2b. Although there is expression of USP2a in HepG2, we have seen more consistent results with USP2b, making it our point of focus. Since we are overexpressing the various isoforms, we want the endogenous expression to be low.

USP2a was found to decrease in HCC compared to normal samples. However, in paired mice and human tumor and surrounding tissues, about half show an increase in USP2a in tumors, while the other half show a decrease. For human samples in particular, we saw both a dramatic increase and decrease. There was no trend for the relationship of USP2a in regards to gender, race, age, histologic grade, pTNM, focality, or tumor size, indicating another factor maybe affecting USP2a. Interestingly, a previous publication found the opposite relationship of USP2a between HCC and

normal samples, with USP2a expression increased in the tumor (21). Considering the dramatic increases and decreases seen in paired surrounding versus tumor tissue, it is probable that another factor affects USP2a, something unidentified in the current study or previous study. We propose this additional factor could be Farnesoid X Receptor (FXR) isoform alpha 2. Interestingly, we noted that FXRα2 was either undetected or at extremely low levels in the samples with low USP2a. It would be an interesting avenue to explore the role of FXR on USP2 expression. In addition to *in vivo* samples, USP2a function was examined in HepG2 cell lines. Overexpression of USP2a displays increased proliferation, colony formation, and wound healing characteristics. It showed minimal effect for migration, and no effect in invasion and apoptosis. This suggests of the 6 hallmarks of cancer, USP2a overexpression in an established HCC cell line allows the cells to have increased replicative potential.

Of great interest, this study has shown that USP2b correlates with healthier liver and decreased levels correlate with HCC surrounding and tumor samples. In human samples, USP2b was significantly decreased in human HCC samples compared to normal liver, and decreased within tumor samples compared to the surrounding liver tissue. Unfortunately, we have limited data about time of collection of samples from human patients. For paired samples, we addressed this uncontrollable factor by comparing percent decrease for each sample so time of day collected would have minimal impact. For normal human liver versus HCC samples, although we have no way to determine time of day samples were collected, there was a dramatic decrease in the HCC samples. Given that both HCC and normal samples were collected randomly through the day, the decrease seen can be taken as a true decrease. Together, this

suggests USP2b correlates with a healthier liver phenotype, and as the state of the liver worsens USP2b also decreases. In functional assays, overexpression of USP2b in HepG2 cells displayed increased proliferation, wound healing, colony formation, migration, invasion, and apoptosis. Interestingly, the overexpression of USP2b in HCC cells showed both tumor-enhancing and tumor-protective functions, such as insensitivity to anti-growth signals like apoptosis.

While USP2b has been identified mostly as a circadian gene with little research into its cancer properties, this study clearly shows an involvement of USP2b with HCC. Although most current literature suggests a solely circadian role, cancer and circadian rhythms are intertwined. Notably, there has been accumulating epidemiological and genetic evidence implicating a connection between cancer development and circadian rhythms (25–27). Epidemiological studies have linked circadian disruption to increased susceptibility of cancer development in all key organ systems in humans, including breast (28), ovarian (29), lung (30), prostate (30), pancreatic (31), colorectal (32), and hepatocellular carcinoma (33). At the molecular level, it has been suggested that points of coupling between the cellular clock and cell cycle exist, thereby affecting genes including c-Myc and cyclin D, suggesting a potential link between cancer and circadian regulation (34).

Although there is a decrease in USP2a in HCC subjects compared to healthy, overall USP2a displays tumor formation properties in HCC. Unlike USP2b, which shows a decrease in all tumors compared to surrounding pairs, USP2a shows an increase in half and a decrease in half for both mice and human samples. As an average, USP2a is increased in tumor samples compared to surrounding since the increases seen are so

dramatic. Additionally, all functional assays for USP2a point to increased tumor-forming properties. The functional assays for USP2b showed both tumor-forming and tumor-protective properties. As discussed, USP2b has other functional characteristics, such as circadian effects. The opposing cancer properties seen in the functional assays may be due to the multifaceted role of USP2b in the cell. Unlike the functional assays, the tumor samples from human and mice were very consistent throughout. USP2b shows a steady decrease in hepatic expression from normal, to surrounding HCC tissue, to HCC tumor tissue. Additionally, all paired tumors showed a decrease in USP2b compared to surrounding tissue. This same trend is seen in paired mice samples, with the majority of samples showing a decrease in USP2b in tumor tissue. Taken together, USP2a and USP2b have opposing roles in HCC development, with USP2a displaying a tumor-promotion role and USP2b displaying a tumor-protective role.

Supplementary Material

Refer to Web version on PubMed Central for supplementary material.

Acknowledgements

Technical and instrumental support from the RI-INBRE Core Facility in the College of Pharmacy is greatly appreciated.

References

1. Cooper GM. Protein Degradation. Cell Mol Approach 2nd Ed [Internet]. 2000 [cited 2018 Jun 6]; Available from: https://www.ncbi.nlm.nih.gov/books/NBK9957/

2. Komander D, Rape M. The Ubiquitin Code. Annu Rev Biochem. 2012;81(1):203–29.

3. Gousseva N, Baker R. Gene structure, alternate splicing, tissue distribution, cellular localization, and developmental expression pattern of mouse deubiquitinating enzyme isoforms Usp2-45 and Usp2-69. Gene Expr. 2003;11(3–4):163–79.

4. Kim J, Kim W-J, Liu Z, Loda M, Freeman MR. The ubiquitin-specific protease USP2a enhances tumor progression by targeting cyclin A1 in bladder cancer. Cell Cycle. 2012 Mar 15;11(6):1123–30.

5. Graner E, Tang D, Rossi S, Baron A, Migita T, Weinstein LJ, et al. The isopeptidase USP2a regulates the stability of fatty acid synthase in prostate cancer. Cancer Cell. 2004 Mar;5(3):253–61.

6. Metzig M, Nickles D, Falschlehner C, Lehmann-Koch J, Straub BK, Roth W, et al. An RNAi screen identifies USP2 as a factor required for TNF-α-induced NF-κB signaling. Int J Cancer. 2011 Aug 1;129(3):607–18.

7. Liu Z, Zanata SM, Kim J, Peterson MA, Di Vizio D, Chirieac LR, et al. The ubiquitin-specific protease USP2a prevents endocytosis-mediated EGFR degradation. Oncogene. 2013 Mar;32(13):1660–9.

8. Yang Y, Hou J, Qu L, Wang G, Ju H, Zhao Z, et al. [Differential expression of USP2, USP14 and UBE4A between ovarian serous cystadenocarcinoma and adjacent normal tissues]. Xi Bao Yu Fen Zi Mian Yi Xue Za Zhi Chin J Cell Mol Immunol. 2007 Jun;23(6):504–6.

9. Marine J-C, Francoz S, Maetens M, Wahl G, Toledo F, Lozano G. Keeping p53 in check: essential and synergistic functions of Mdm2 and Mdm4. Cell Death Differ. 2006 Jun;13(6):927–34.

10. Stevenson LF, Sparks A, Allende-Vega N, Xirodimas DP, Lane DP, Saville MK. The deubiquitinating enzyme USP2a regulates the p53 pathway by targeting Mdm2. EMBO J. 2007 Feb 21;26(4):976–86.

11. Allende-Vega N, Sparks A, Lane DP, Saville MK. MdmX is a substrate for the deubiquitinating enzyme USP2a. Oncogene. 2010 Jan;29(3):432–41.

12. Benassi B, Flavin R, Marchionni L, Zanata S, Pan Y, Chowdhury D, et al. MYC Is Activated by USP2a-Mediated Modulation of MicroRNAs in Prostate Cancer. Cancer Discov. 2012 Mar;2(3):236–47.

13. Storch K-F, Lipan O, Leykin I, Viswanathan N, Davis FC, Wong WH, et al. Extensive and divergent circadian gene expression in liver and heart. Nature. 2002 May;417(6884):78–83.

14. Yan J, Wang H, Liu Y, Shao C. Analysis of Gene Regulatory Networks in the Mammalian Circadian Rhythm. PLoS Comput Biol [Internet]. 2008 Oct 10 [cited 2018 May 20];4(10). Available from: https://www.ncbi.nlm.nih.gov/pmc/articles/PMC2543109/

15. Yu EA, Weaver DR. Disrupting the circadian clock: Gene-specific effects on aging, cancer, and other phenotypes. Aging. 2011 May 1;3(5):479–93.

16. Scoma HD, Humby M, Yadav G, Zhang Q, Fogerty J, Besharse JC. The de-ubiquitinylating enzyme, USP2, is associated with the circadian clockwork and regulates its sensitivity to light. PloS One. 2011;6(9):e25382.

17. Yang Y, Duguay D, Fahrenkrug J, Cermakian N, Wing SS. USP2 Regulates the Intracellular Localization of PER1 and Circadian Gene Expression. J Biol Rhythms. 2014 Aug;29(4):243–56.

18. Tong X, Buelow K, Guha A, Rausch R, Yin L. USP2a Protein Deubiquitinates and Stabilizes the Circadian Protein CRY1 in Response to Inflammatory Signals. J Biol Chem. 2012 Jul 20;287(30):25280–91.

19. Gewies A, Grimm S. UBP41 is a proapoptotic ubiquitin-specific protease. Cancer Res. 2003 Feb 1;63(3):682–8.

20. Mahul-Mellier A-L, Datler C, Pazarentzos E, Lin B, Chaisaklert W, Abuali G, et al. De-ubiquitinating proteases USP2a and USP2c cause apoptosis by stabilising RIP1. Biochim Biophys Acta BBA - Mol Cell Res. 2012 Aug;1823(8):1353–65.

21. Calvisi DF, Wang C, Ho C, Ladu S, Lee SA, Mattu S, et al. Increased lipogenesis, induced by AKT-mTORC1-RPS6 signaling, promotes development of human hepatocellular carcinoma. Gastroenterology. 2011 Mar;140(3):1071-1083.e5.

22. Hanahan D, Weinberg RA. The Hallmarks of Cancer. Cell. 2000 Jan 7;100(1):57–70.

23. Menyhárt O, Harami-Papp H, Sukumar S, Schäfer R, Magnani L, de Barrios O, et al. Guidelines for the selection of functional assays to evaluate the hallmarks of cancer. Biochim Biophys Acta BBA - Rev Cancer. 2016 Dec 1;1866(2):300–19.

24. Kramer N, Walzl A, Unger C, Rosner M, Krupitza G, Hengstschläger M, et al. In vitro cell migration and invasion assays. Mutat Res Mutat Res. 2013 Jan 1;752(1):10–24.

25. Fu L, Kettner NM. The circadian clock in cancer development and therapy. Vol. 119, Progress in Molecular Biology and Translational Science. 2013. p. 221–82.

26. Sahar S, Sassone-Corsi P. Metabolism and cancer: the circadian clock connection. Nat Rev Cancer. 2009;9(12):886–96.

27. Gery S, Koeffler HP. Circadian rhythms and cancer. Vol. 9, Cell Cycle. 2010. p. 1097–103.

28. Stevens RG. Working against our endogenous circadian clock: Breast cancer and electric lighting in the modern world. Mutat Res - Genet Toxicol Environ Mutagen. 2009;679(1–2):6–8.

29. Touitou Y, Bogdan A, Lévi F, Benavides M, Auzéby A. Disruption of the circadian patterns of serum cortisol in breast and ovarian cancer patients: relationships with tumour marker antigens. Br J Cancer. 1996;74(8):1248–52.

30. Kloog I, Haim A, Stevens RG, Portnov BA. Global co-distribution of light at night (LAN) and cancers of prostate, colon, and lung in men. Chronobiol Int. 2009;26(1):108–25.

31. Relles D, Sendecki J, Chipitsyna G, Hyslop T, Yeo CJ, Arafat HA. Circadian gene expression and clinicopathologic correlates in pancreatic cancer. J Gastrointest Surg Off J Soc Surg Aliment Tract. 2013 Mar;17(3):443–50.

32. Schernhammer ES, Laden F, Speizer FE, Willett WC, Hunter DJ, Kawachi I, et al. Night-shift work and risk of colorectal cancer in the nurses' health study. J Natl Cancer Inst. 2003;95(11):825–8.

33. Buzzelli G, Dattolo P, Pinzani M, Brocchi A, Romano S, Gentilini P. Circulating growth hormone and insulin-like growth factor-I in nonalcoholic liver cirrhosis with or without superimposed hepatocarcinoma: evidence of an altered circadian rhythm. Am J Gastroenterol. 1993 Oct;88(10):1744–8.

34. Kelleher FC, Rao A, Maguire A. Circadian molecular clocks and cancer. Vol. 342, Cancer Letters. 2014. p. 9–18.

Fig. 1 A

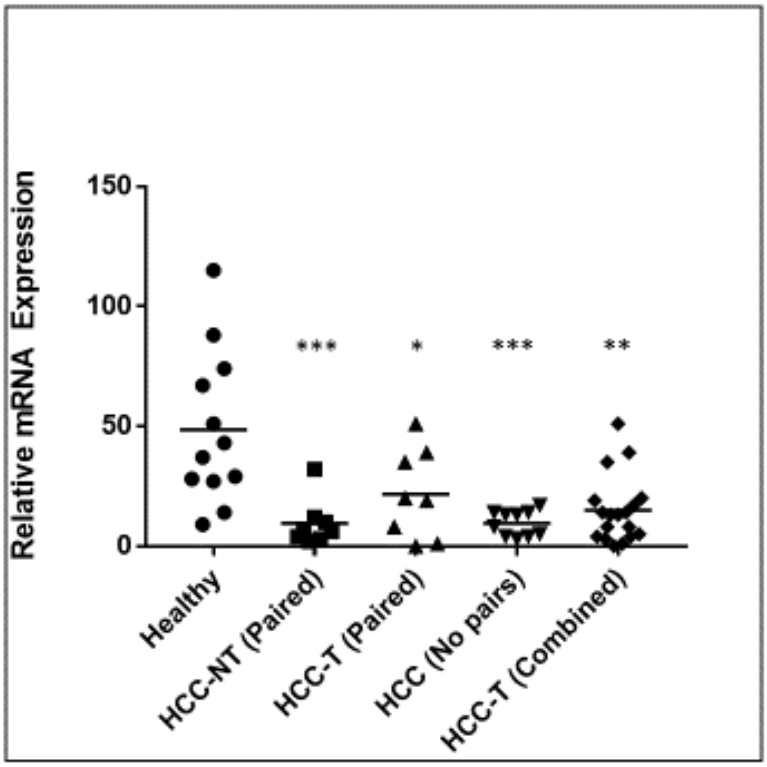
Relative mRNA Expression
150
100
50
0
***
*
***
**
Healthy
HCC-NT (Paired)
HCC-T (Paired)
HCC (No pairs)
HCC-T (Combined)

Fig. 1 B

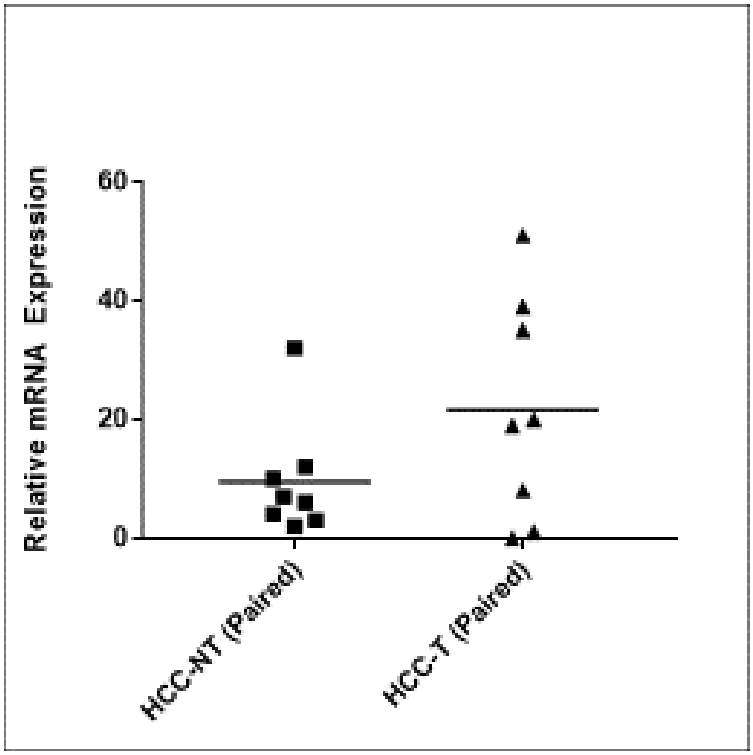
Relative mRNA Expression
60
40
20
0
HCC-NT (Paired)
HCC-T (Paired)

Fig. 1 C

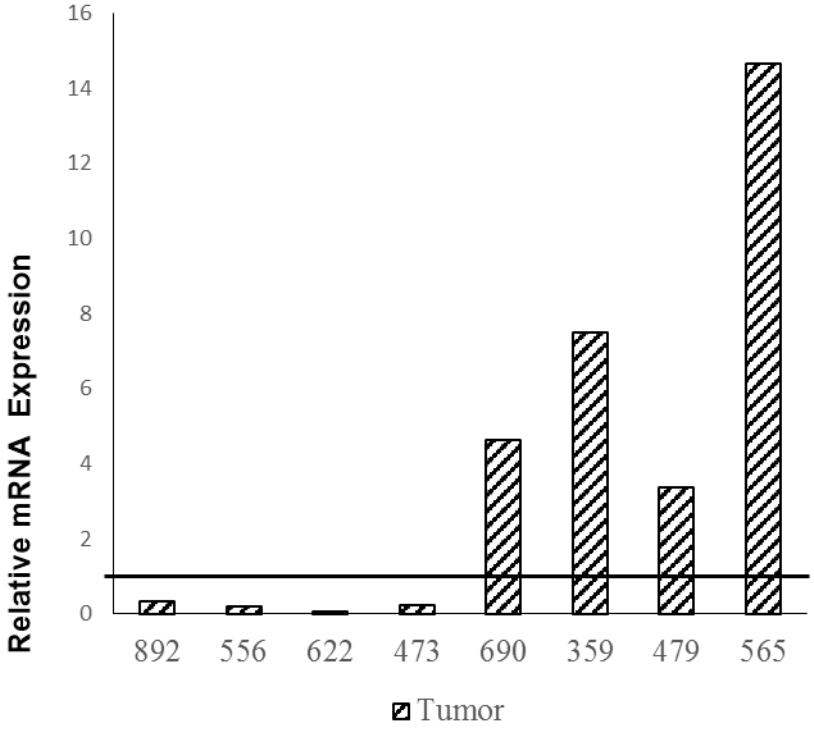
Relative mRNA Expression
16
14
12
10
8
6
4
2
0
892
556
622
473
690
359
479
565
Tumor

Fig. 2 A

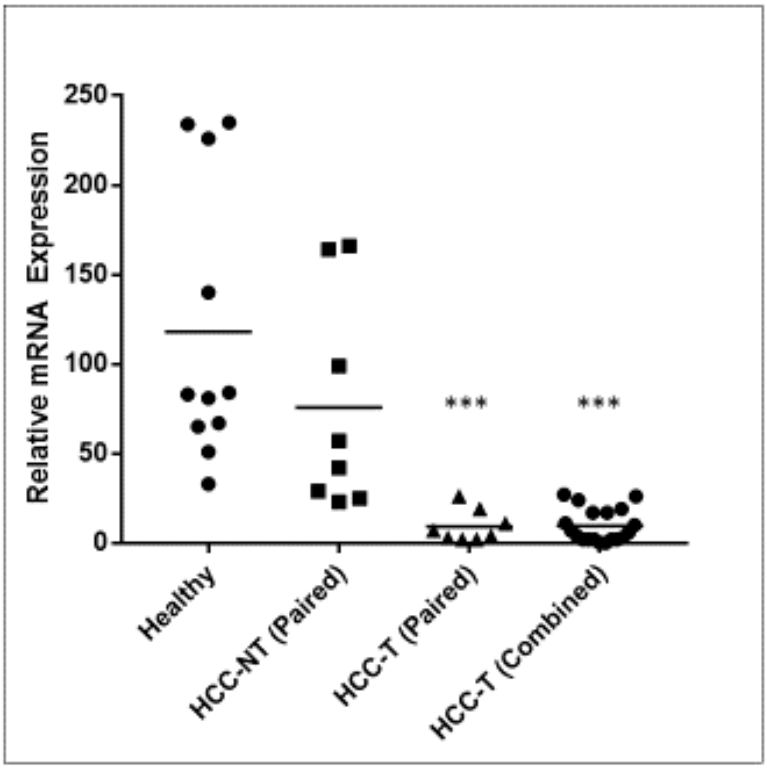
Relative mRNA Expression
250
200
150
100
50
0
***
***
Healthy
HCC-NT (Paired)
HCC-T (Paired)
HCC-T (Combined)

Fig. 2 B

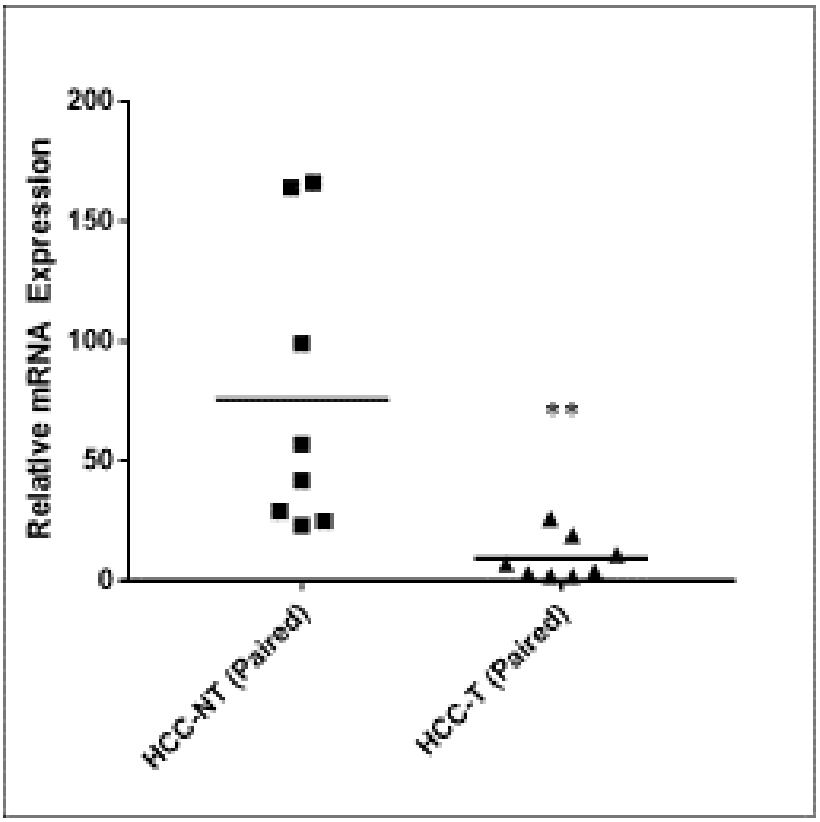
Relative mRNA Expression
200
150
100
50
0
**
HCC-NT (Paired)
HCC-T (Paired)

Fig. 2 C

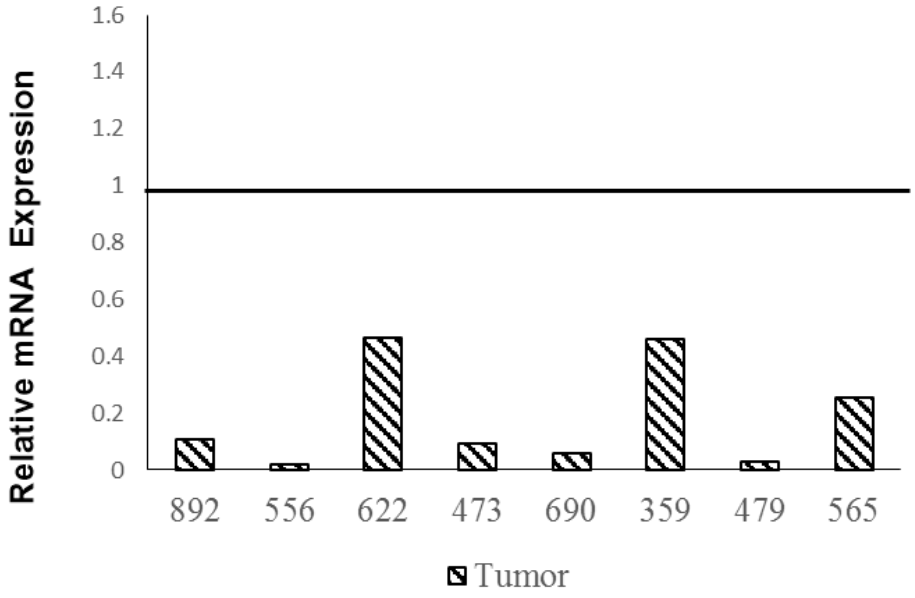
Relative mRNA Expression
1.6
1.4
1.2
1
0.8
0.6
0.4
0.2
0
892
556
622
473
690
359
479
565
Tumor

Fig. 2 D

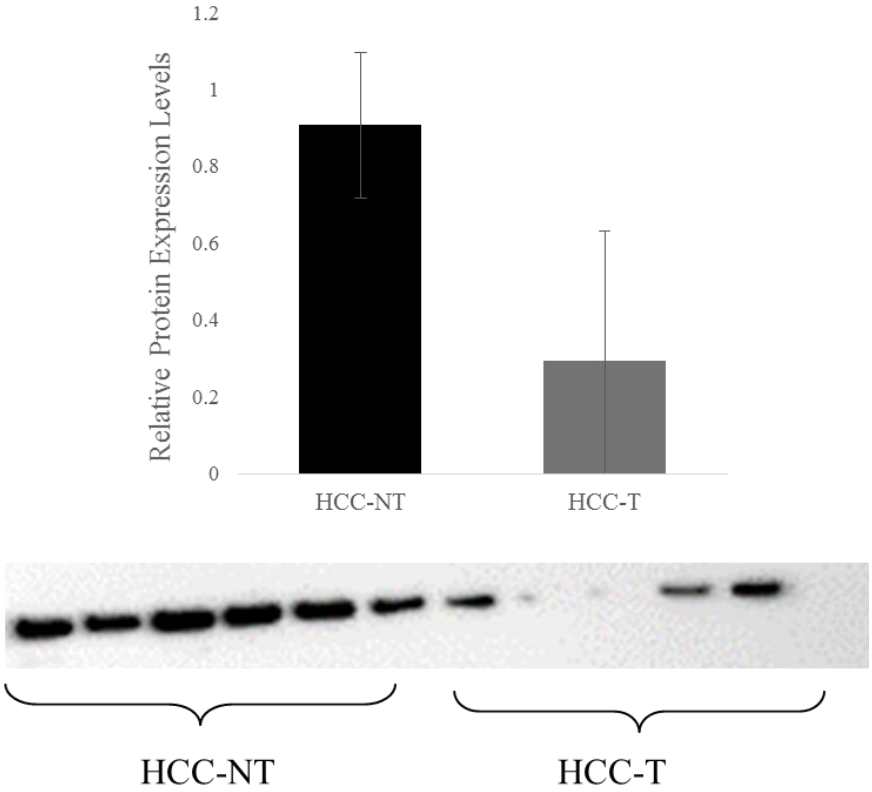

Fig. 3

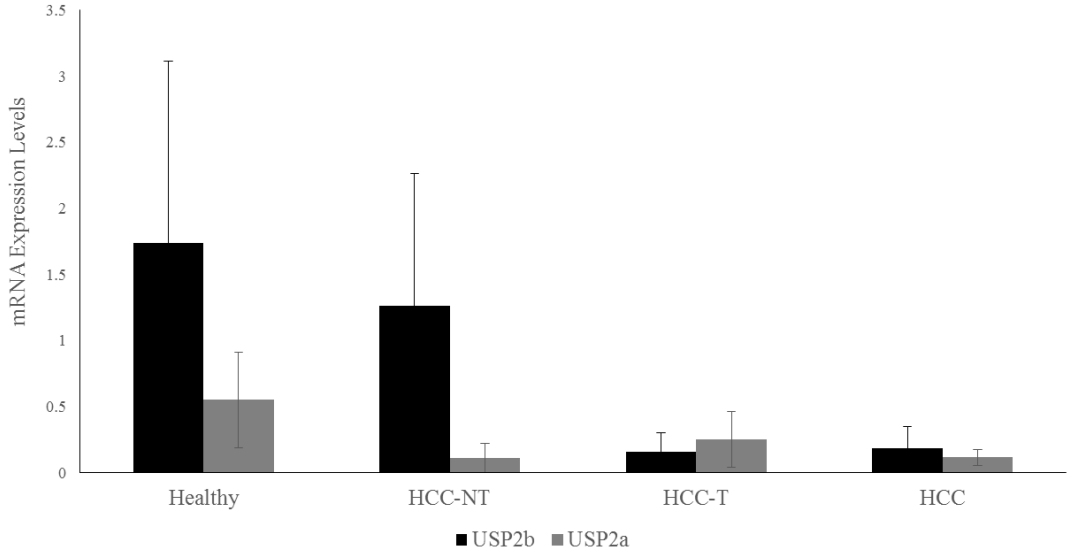

	ΔCT			
	Healthy	HCC-NT	HCC-T	HCC
USP2a	**6.5**	**9.0**	**8.4**	**8.7**
USP2b	**5.0**	**5.4**	**8.6**	**8.5**

Fig. 4

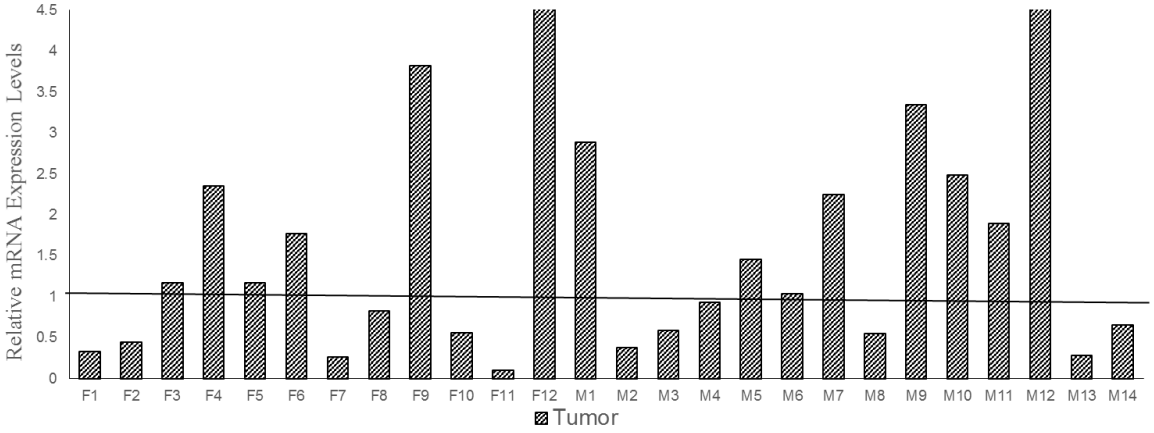
Relative mRNA Expression Levels
4.5
4
3.5
3
2.5
2
1.5
1
0.5
0
F1 F2 F3 F4 F5 F6 F7 F8 F9 F10 F11 F12 M1 M2 M3 M4 M5 M6 M7 M8 M9 M10 M11 M12 M13 M14
Tumor

Fig. 5

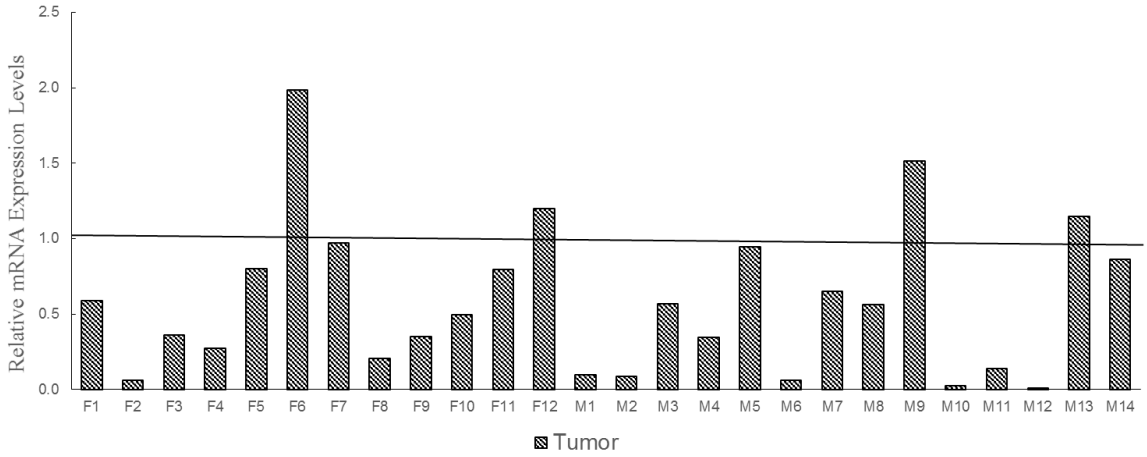
Relative mRNA Expression Levels
2.5
2.0
1.5
1.0
0.5
0.0
F1 F2 F3 F4 F5 F6 F7 F8 F9 F10 F11 F12 M1 M2 M3 M4 M5 M6 M7 M8 M9 M10 M11 M12 M13 M14
Tumor

Fig. 6

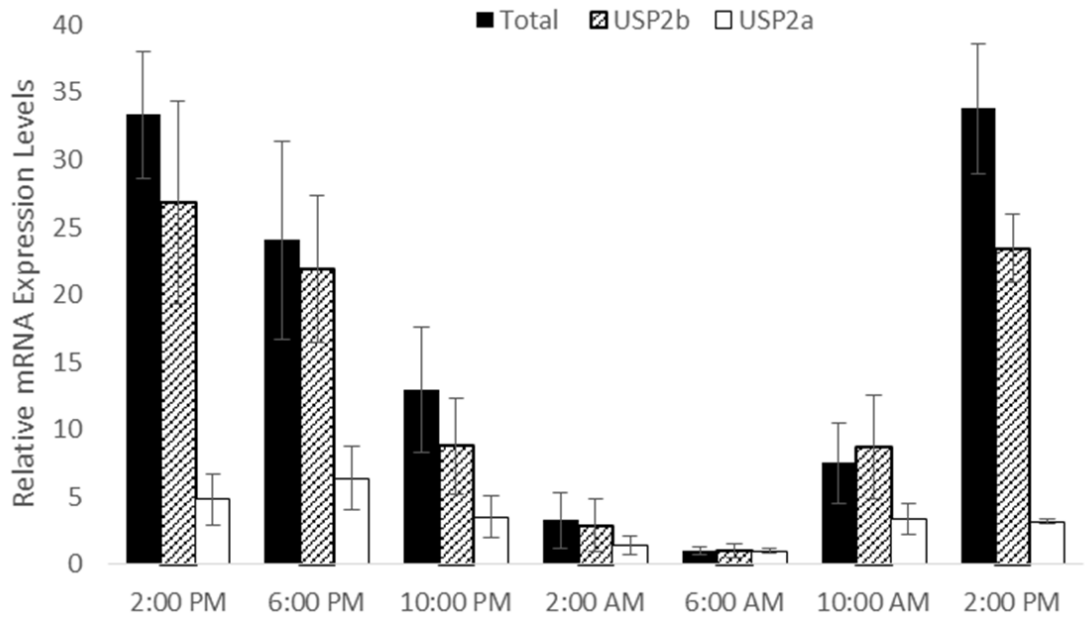

	ΔCT						
	2:00pm	6:00pm	10:00pm	2:00am	6:00am	10:00am	2:00pm
USP2a	10.76	11.02	11.94	13.13	13.55	11.97	11.88
USP2b	6.45	6.92	8.16	10.21	11.38	8.58	6.85
Total USP2	6.51	6.90	8.02	10.33	11.46	8.64	6.64

Fig. 7 A & B

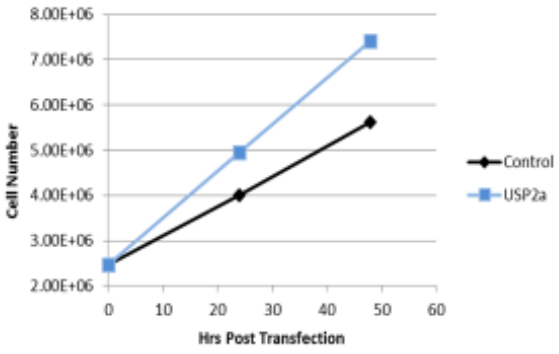

24hrs: 25% increase**
48hrs: 30% increase**

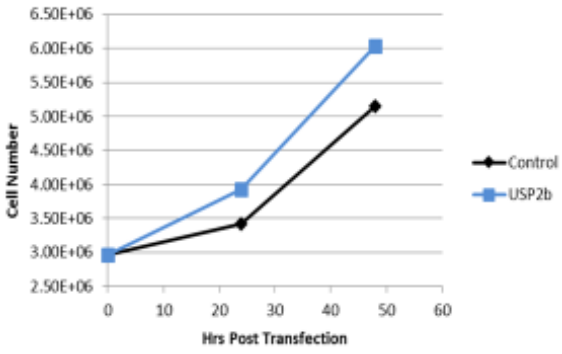

24hrs: 15% increase*
48hrs: 20% increase**

Fig. 7 C

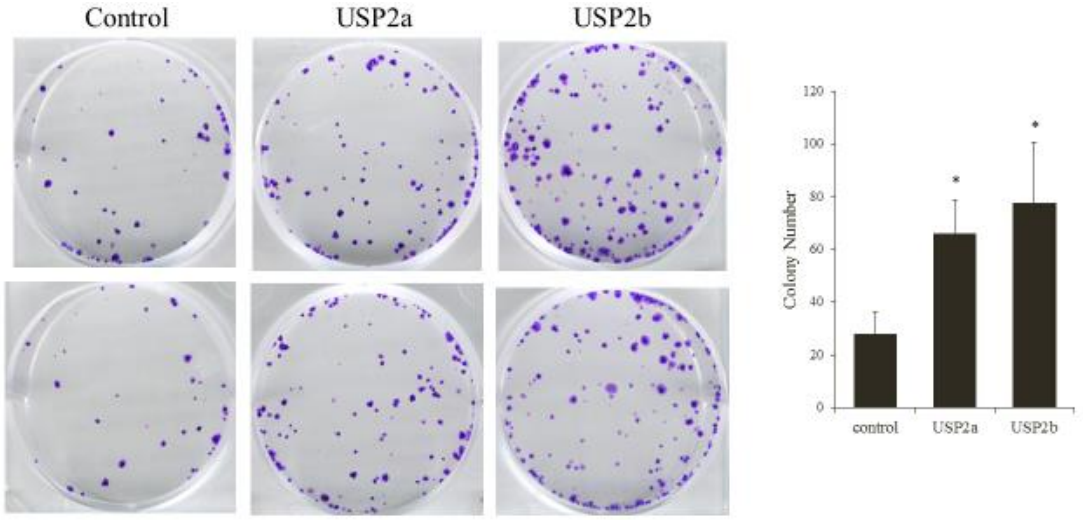

Fig. 7 D

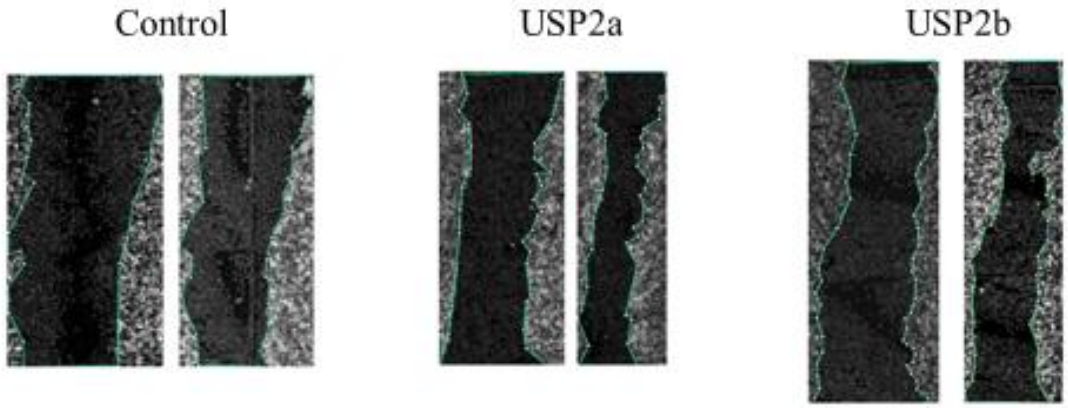

Average % Wound Closure:
Control: 21.33%
USP2a: 32.33%*
USP2b: 29.33%*

Fig. 8 A

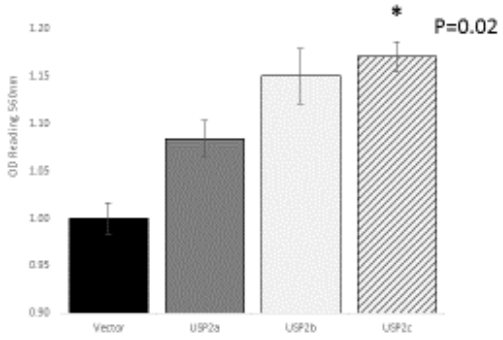

						ave	stdeva	norm	% Δ
V	0.266117	0.28452	0.252168		Vector	0.267602	0.016227	1.00	0.0
A	0.284671	0.274344	0.311223		USP2a	0.290079	0.019025	1.08	8.4
B	0.340539	0.297991	0.284655		USP2b	0.307728	0.029187	1.15	15.0
C	0.305332	0.302459	0.331815		USP2c	0.313202	0.016183	1.17	17.0

Fig. 8 B

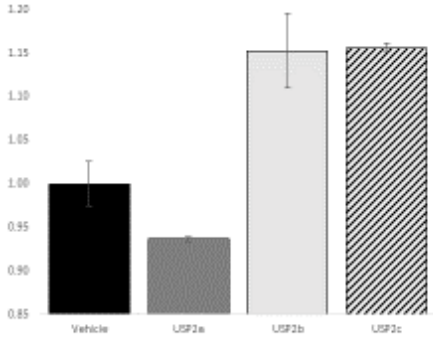

						ave	stdeva	norm	% Δ
Vehicle	0.24023	0.275348	0.291008		Vehicle	0.268862	0.026003	1.00	0.0
USP2a	0.254436	0.248827	0.252164		USP2a	0.251809	0.002821	0.94	-6.3
USP2b	0.263621	0.348048	0.317811		USP2b	0.309826	0.042776	1.15	15.2
USP2c	0.305024	0.314479	0.31286		USP2c	0.310788	0.005057	1.16	15.6

Fig. 8 C

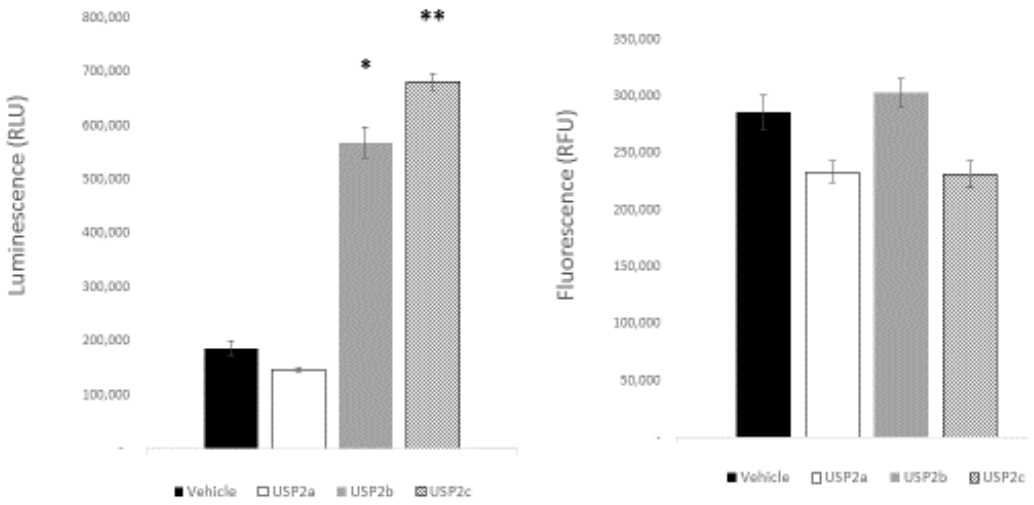
Luminescence (RLU)
800,000
700,000
600,000
500,000
400,000
300,000
200,000
100,000
-
*
**
Vehicle
USP2a
USP2b
USP2c
Fluorescence (RFU)
350,000
300,000
250,000
200,000
150,000
100,000
50,000
-
Vehicle
USP2a
USP2b
USP2c

FIGURE LEGENDS

Fig. 1. USP2a mRNA levels in Healthy Liver and HCC patients. Human samples were divided into healthy, HCC-NT (paired), HCC-T (paired), HCC no pairs, and HCC combined. A single asterisk (*) indicates $p<0.05$, double asterisk (**) indicates $p<0.01$, and a triple asterisk (***) indicates $p<0.001$. (A) A statistically significant decrease in USP2a mRNA is seen in all sample groups compared to healthy tissue. (B) Paired HCC-NT and HCC-T displayed an overall increase in USP2a mRNA within the tumor. (C) When normalized to individual samples, half of the samples displayed a dramatic increase while the other had a dramatic decrease. The line represents the surrounding tissue and the bar represents the tumor.

Fig. 2. USP2b mRNA and protein levels decrease in Healthy Liver and HCC patients. Human samples were divided into healthy, HCC-NT (paired), HCC-T (paired), and HCC combined. A single asterisk (*) indicates $p<0.05$, double asterisk (**) indicates $p<0.01$, and a triple asterisk (***) indicates $p<0.001$. (A) A statistically significant decrease is seen between USP2b mRNA from healthy to HCC-T and again healthy to HCC-T (combined). (B) Paired HCC-NT and HCC-T displayed an overall decrease in USP2b mRNA within the tumor. (C) When normalized to individual samples, all showed a dramatic decrease in USP2b. The line represents the surrounding tissue and the bar represents the tumor. (D) Of the 8 paired samples, 6 were available for protein analysis. A significant decrease in USP2b protein is seen in HCC-T samples compared to HCC-NT.

Fig. 3. Delta CT Values for USP2a and USP2b in Healthy Liver and HCC Patients. Delta CT values were analyzed to determine relative abundance of the two isoforms. The smaller the value, the more abundant the mRNA. Overall, USP2b is more abundant in healthy and HCC-NT samples compared to USP2a. Within HCC tumor samples, abundance of the two isoforms is comparable. The line represents the surrounding tissue and the bar represents the tumor.

Fig. 4. USP2a expression levels in Murine Surrounding Liver and Tumor Samples. USP2a mRNA is dysregulated in murine tumor compared to surrounding tissue. In 14 of the 26 samples there is an increase, while the other 12 show a decrease. The line represents the surrounding tissue and the bar represents the tumor.

Fig. 5. USP2b expression decreases in Murine Surrounding Liver and Tumor Samples. USP2b mRNA is decreased in murine tumor compared to surrounding tissue. Of the 26 samples, 22 displayed a decrease. The line represents the surrounding tissue and the bar represents the tumor.

Fig. 6. Circadian Pattern of USP2 mRNA in Healthy Mice Liver. Total USP2, USP2a, and USP2b mRNA levels were analyzed every 4 hours for 24 hours in healthy wild type mice samples. The total USP2 and USP2b probe displayed similar abundance, as displayed in the change in CT values, while USP2a was less abundant. Additionally, it is important to note from this figure the total USP2 probe follows the same trend as USP2b, as this is the more abundant isoform in the mouse liver.

Fig. 7. USP2a and USP2b Increases Proliferation, Wound Healing, and Colony Formation. HepG2 cells were transfected with USP2a or USP2b. A single asterisk (*) indicates $p<0.05$ and a double asterisk (**) indicates $p<0.01$. (A) Cells were counted 24 and 48 hours post transfection with USP2a and (B) USP2b. (C) Cells were seeded at a low density of 600 cells in a 6 well plate and allowed to grow for 2 weeks. A statistically significant increase in colony number was seen in USP2a and USP2b transfected wells. (D) A scratch was taken in a monolayer of serum starved USP2 transfected HepG2 cells. Images were taken at time of initial wound (left) and 48 hours post scratch (right). Average % wound closure was measured from 3 random fields. Both USP2a and USP2b lead to a statistically significant increase in wound closure

Fig. 8. Increased Migration, Invasion, and Apoptosis of USP2b and USP2c in HepG2 Cells. A single asterisk (*) indicates $p<0.05$ and a triple asterisk (***) indicates $p<0.001$. HepG2 cells were transfected with USP2a, USP2b, or USP2b. Cells were then seeded in an 8μm pore chamber for (A) migration or (B) invasion chamber with ECM in triplicate. Media containing 20% FBS was used on opposing side of the membrane. An increase in both (A) migration and (B) invasion was seen for both USP2b and USP2c. (C) Cells were seeded into a 96 well plate, transfected, and RealTime-Glo Annexin V Apoptosis and Necrosis detection media was added. Luminescence and fluorescence were measured to detect apoptosis and necrosis, respectively. A significant increase in apoptosis was seen for USP2b and USP2c.

SUPPLEMENT TABLES

Supplementary table 1: Sequence information for human USP2A, UPS2, and USP2C plasmid constructs in pcDNA3.1(+) vector.

USP2A (NM_004205)
aagcttgccgccaccATGTCCCAGCTGAGCAGCACACTGAAGAGATACACCGAG
AGCGCCAGGTACACAGATGCCCACTACGCCAAGTCCGGCTACGGCGCTT
ACACACCTAGCTCCTACGGCGCCAACCTGGCCGCTAGCCTGCTGGAAAA
GGAGAAGCTGGGCTTTAAGCCCGTGCCTACATCCAGCTTTCTGACCAGA
CCCAGAACCTACGGCCCCAGCTCCCTGCTGGACTACGACAGAGGCAGGC
CTCTGCTGAGACCTGATATCACCGGCGGCGGCAAGAGGGCCGAGTCTCA
AACCAGGGGCACAGAGAGACCCCTGGGCTCCGGACTGAGCGGAGGATC
TGGCTTTCCTTACGGCGTGACAAATAATTGTCTGTCCTACCTGCCCATCA
ATGCCTACGACCAGGGCGTGACACTGACCCAGAAGCTGGACAGCCAGTC
CGACCTGGCCAGGGACTTTAGCTCCCTGAGGACCTCCGATTCCTACAGA
ATCGATCCTAGAAATCTGGGCAGGTCCCCCATGCTGGCCAGGACAAGGA
AGGAGCTGTGCACCCTGCAGGGCCTGTACCAGACAGCCTCCTGCCCTGA
GTACCTGGTGGACTACCTGGAGAATTACGGCAGAAAGGGCAGCGCCTCC
CAGGTGCCTTCCCAGGCTCCTCCAAGCAGAGTGCCTGAGATCATCTCCCC
CACCTACAGACCCATCGGCAGGTACACCCTGTGGGAGACCGGCAAGGGC
CAGGCTCCAGGACCATCCAGATCCAGCTCCCCCGGCAGAGACGGCATGA
ATTCCAAGTCCGCCCAGGGCCTGGCCGGCCTGAGGAACCTGGGAAATAC
ATGTTTCATGAATAGCATCCTGCAGTGTCTGAGCAACACCAGAGAGCTG

AGGGACTACTGCCTGCAGAGACTGTACATGAGGGATCTGCACCACGGCA GCAATGCCCACACCGCCCTGGTGGAGGAGTTTGCCAAGCTGATCCAGAC CATCTGGACCTCCAGCCCTAACGATGTGGTGTCCCCCTCCGAGTTCAAGA CCCAGATCCAGAGATACGCCCCTAGATTCGTGGGCTACAATCAGCAGGA CGCCCAGGAGTTTCTGAGATTTCTGCTGGATGGCCTGCACAACGAGGTG AATAGGGTGACCCTGAGACCTAAGAGCAATCCTGAGAACCTGGATCACC TGCCTGACGACGAGAAGGGCAGGCAGATGTGGAGAAAGTACCTGGAGA GAGAGGACTCCAGGATCGGCGATCTGTTCGTGGGCCAGCTGAAGTCCAG CCTGACCTGCACCGACTGCGGCTACTGCTCCACCGTGTTCGACCCCTTCT GGGATCTGAGCCTGCCTATCGCCAAGAGAGGCTACCCCGAGGTGACACT GATGGACTGTATGAGGCTGTTCACCAAGGAGGACGTGCTGGACGGCGAT GAGAAGCCTACCTGTTGCAGATGTAGGGGCAGGAAGAGGTGTATCAAG AAGTTTTCCATCCAGAGGTTTCCCAAGATCCTGGTGCTGCACCTGAAGAG GTTTAGCGAGTCCAGAATCAGAACCAGCAAGCTGACCACATTCGTGAAC TTTCCCCTGAGGGATCTGGATCTGAGGGAGTTCGCCTCCGAGAATACCA ACCACGCCGTGTACAATCTGTACGCCGTGTCCAACCACTCCGGCACCAC CATGGGCGGCCACTACACAGCCTACTGCAGATCCCCCGGCACAGGCGAG TGGCACACATTTAACGATAGCAGCGTGACCCCCATGAGCTCCAGCCAGG TGAGGACCAGCGACGCCTACCTGCTGTTCTACGAGCTGGCCTCCCCCCCT TCCAGAATGTGAggatcc
USP2B (NM_171997)

aagcttgccgccaccATGAGAACATCCTACACAGTGACCCTGCCCGAGGACCCCC

CCGCTGCTCCTTTTCCAGCCCTGGCTAAGGAGCTGAGGCCTAGAAGCCCT

CTGTCCCCTAGCCTGCTGCTGAGCACATTTGTGGGCCTGCTGCTGAATAA

GGCCAAGAATAGCAAGTCCGCCCAGGGCCTGGCCGGCCTGAGGAACCTG

GGAAACACATGTTTTATGAATAGCATCCTGCAGTGCCTGTCCAACACAA

GGGAGCTGAGAGATTACTGCCTGCAGAGACTGTACATGAGGGACCTGCA

CCACGGCAGCAATGCCCACACCGCCCTGGTGGAGGAGTTTGCCAAGCTG

ATCCAGACAATCTGGACAAGCAGCCCCAACGATGTGGTGAGCCCTTCCG

AGTTCAAGACACAGATCCAGAGATACGCCCCTAGATTTGTGGGCTACAA

CCAGCAGGACGCCCAGGAGTTTCTGAGATTCCTGCTGGATGGCCTGCAC

AACGAGGTGAACAGAGTGACACTGAGGCCCAAGTCCAATCCCGAGAAT

CTGGATCACCTGCCTGATGACGAGAAGGGCAGACAGATGTGGAGAAAG

TACCTGGAGAGAGAGGACTCCAGGATCGGCGATCTGTTCGTGGGCCAGC

TGAAGTCCTCCCTGACATGTACAGATTGTGGCTACTGCAGCACCGTGTTC

GACCCCTTTTGGGACCTGAGCCTGCCCATCGCCAAGAGGGGCTACCCTG

AGGTGACCCTGATGGACTGCATGAGGCTGTTTACAAAGGAGGATGTGCT

GGATGGCGACGAGAAGCCTACCTGCTGCAGATGCAGAGGCAGAAAGAG

ATGTATCAAGAAGTTTTCCATCCAGAGGTTCCCCAAGATCCTGGTGCTGC

ACCTGAAGAGGTTCAGCGAGTCCAGAATCAGAACAAGCAAGCTGACCA

CATTCGTGAATTTCCCTCTGAGAGATCTGGACCTGAGAGAGTTTGCCTCC

GAGAATACCAATCACGCCGTGTACAACCTGTACGCCGTGAGCAATCACT

CCGGCACCACAATGGGCGGCCACTACACCGCCTACTGCAGATCCCCCGG

CACCGGAGAGTGGCACACCTTTAATGATAGCTCCGTGACCCCCATGAGC

TCCTCCCAGGTGAGGACATCCGACGCCTACCTGCTCTTCTACGAGCTGGC CAGCCCCCCTTCCAGGATGTGAggatcc
USP2C (NM_001243759)
aagcttgccgccaccATGCTGGTGCCTGGCTCCACCAGGCCATACTCCAAGAAGA GGCAGAATAGCAAGAGCGCCCAGGGCCTGGCCGGCCTGAGGAACCTGG GAAATACATGTTTCATGAACTCCATCCTGCAGTGCCTGTCCAATACCAGA GAGCTGAGGGATTACTGTCTGCAGAGGCTGTACATGAGGGATCTGCACC ACGGCTCCAACGCCCACACCGCTCTGGTGGAGGAGTTCGCCAAGCTGAT CCAGACAATCTGGACCTCCTCCCCTAACGATGTGGTGTCCCCTAGCGAGT TTAAGACACAGATCCAGAGATACGCCCCTAGGTTCGTGGGCTACAACCA GCAGGATGCCCAGGAGTTCCTGAGGTTCCTGCTGGACGGCCTGCACAAT GAGGTGAACAGAGTGACACTGAGACCTAAGTCCAATCCCGAGAACCTGG ACCACCTGCCTGATGACGAGAAGGGCAGACAGATGTGGAGAAAGTACC TGGAGAGGGAGGATTCCAGAATCGGCGACCTGTTCGTGGGCCAGCTGAA GTCCTCCCTGACCTGTACCGACTGCGGCTACTGCAGCACCGTGTTCGACC CTTTTTGGGACCTGAGCCTGCCCATCGCCAAGAGGGGCTACCCTGAGGT GACACTGATGGACTGTATGAGGCTGTTCACAAAGGAGGATGTGCTGGAT GGCGACGAGAAGCCTACCTGTTGCAGGTGCAGGGGCAGGAAGAGATGC ATCAAGAAGTTTAGCATCCAGAGGTTTCCCAAGATCCTGGTGCTGCACCT GAAGAGGTTTAGCGAGTCCAGAATCAGAACCTCCAAGCTGACCACATTC GTGAACTTCCCCCTGAGAGATCTGGACCTGAGAGAGTTTGCCTCCGAGA ATACAAACCACGCCGTGTACAATCTGTACGCCGTGTCCAATCACTCCGG

CACCACCATGGGCGGCCACTACACAGCCTACTGCAGGTCCCCCGGCACA

GGCGAATGGCACACCTTTAACGATAGCAGCGTGACCCCTATGAGCTCCT

CCCAGGTGAGGACCAGCGACGCCTACCTGCTGTTTTACGAGCTGGCCTC

CCCCCCTTCCAGAATGTGAggatcc

Supplement Table 2. Patients with pair of HCC-T and HCC-NT samples

ID# [a]	Gender [b]	Race [c]	Age	Histologic Grades	Focality	Tumor Size	Radiation/ Chemo
MAD06-690	F	W	75	G2	Multiple	11.8cm	No
MAD07-622	M	W	53	G1	Solitary	6.8cm	No
MAD08-473	F	W	18	G1	Solitary	9.2cm	No
MAD09-359	F	W	45	N/A[d]	Solitary	12.1cm	No
MAD10-565	M	B	60	G1	Solitary	8.7cm	No
4080892A/B	M	B	1	N/A	Solitary	4.0cm	N/A
4110556A/B	F	B	68	G2/G3	Solitary	5.0cm	N/A
4101479A/B	F	W	69	G2	Solitary	3.5cm	N/A

Note: [a] The top 5 pairs of samples were from University of Virginia, CHTN Mid-Atlantic Division and the bottom 3 pairs of samples were from Ohio State University, CHTN Midwestern Division; [b] F, female and M, male; [c] W, white and B, black; [d] N/A, information not available.

Supplement Table 3. Patients with HCC-T samples

ID# [a]	Gender [b]	Race [c]	Age	Histologic Grades	Focality	Tumor Size	Radiation/ Chemo
51213-T	M	W	78	G2/G3	Solitary	5.0cm	N/A
38403-A	M	B	75	G3	Solitary	6.1cm	No
45167-A	M	W	70	N/A[d]	Multiple	11.0cm	No
46728-A	M	W	70	G1	Solitary	9.0cm	No
47124-A	F	W	32	G1	Solitary	9.0cm	N/A
47419-A	F	B	73	G3	Multiple	5.4cm	No
47715-A	M	W	61	G2/G3	Solitary	3.9cm	No
52875-T	F	W	68	G1	Solitary	8,3cm	No
1110774A	F	B	59	G2	Solitary	4.0cm	N/A
1110926A	M	W	76	G2	Multiple	4.0cm	N/A

Note: [a] The top 8 samples were from University of Pennsylvania, CHTN East Division and the bottom 2 samples were from Ohio State University, CHTN Midwestern Division; [b] F, female and M, male; [c] W, white and B, black; [d] N/A, Information not available.

MANUSCRIPT – 2

Regulation of Ubiquitin Specific Peptidase 2 by Farnesoid X Receptor: Mechanisms and Implications in the Pathogenesis of Hepatocellular Carcinoma

Christina Nadolny, Yuan Chen, and Ruitang Deng

(Prepared for submission Hepatology)

Regulation of Ubiquitin Specific Peptidase 2 by Farnesoid X Receptor: Mechanisms and Implications in the Pathogenesis of Hepatocellular Carcinoma

Christina Nadolny, Yuan Chen, and Ruitang Deng

Department of Biomedical and Pharmaceutical Sciences, Center for Pharmacogenomics and Molecular Therapy, College of Pharmacy, University of Rhode Island, 7 Greenhouse Road, Kingston, RI 02881

Christina Nadolny: cnadolny@my.uri.edu

Yuan Chen: chenyuan@uri.edu

Ruitang Deng: dengr@uri.edu

Key Words: USP2, HCC, FXR, Liver, Deubiquitin

FOOTNOTES

Contact Information:

Ruitang Deng**,** Department of Biomedical and Pharmaceutical Sciences, Center for Pharmacogenomics and Molecular Therapy, College of Pharmacy, University of Rhode Island, Kingston, RI 02881. Tel: 401-874-4950. Fax: 401-874-5787. Email: dengr@uri.edu

Abbreviations:

HCC: Hepatocellular Carcinoma

FXR: Farnesoid X Receptor

USP2: Ubiquitin Specific Peptidase 2

DUB: Deubiquitinating enzyme

MDM2: Murine Double Minute 2

FASN: Fatty Acid Synthetase

RIP1: Receptor-Interacting Serine/Threonine-Protein Kinase 1

PER: Period

OCA: Obeticholic Acid

NASH: Nonalcoholic Steatohepatitis

DMEM: Dulbecco's Modified Eagle Medium

MEM: Minimum Essential Media

FBS: Fetal Bovine Serum

NEAA: Non-Essential Amino Acids

DMSO: Dimethyl Sulfoxide

CDCA: Chenodeoxycholic Acid

PCR: Polymerase Chain Reaction

GAPDH: Glyceraldehyde-3-phosphate Dehydrogenase

PMSF: Phenylmethylsulfonyl Fluoride

PVDF: Polyvinylidene Difluoride

Financial Support:

This work was supported by the National Institutes of Health Grants R01DK087755 and R01CA213419. Additional support for CN was provided by the American Foundation for Pharmaceutical Education (AFPE) Pre-Doctoral Award in Pharmaceutical Sciences.

ABSTRACT

Previously, Ubiquitin Specific Peptidase 2 (USP2) has been identified as a gene of interest in circadian patterns, metabolism, and cancer. Here, we present a novel potential mechanism for USP2 regulation in the liver and in hepatocellular carcinoma (HCC) development through Farnesoid X Receptor (FXR). Between wild type and FXR-/- mice, there was a dysregulation in USP2 and previously identified downstream targets. To determine if the changes in USP2 were due to FXR regulation, we activated FXR in wild type mice, over-expressed FXR in liver cancer cells, and evaluated the effects of FXR activation on the USP2 promoter. Upon treatment with FXR agonist in wild type mice, USP2 mRNA and protein significantly increased compared to vehicle. Additionally, transfection and activation of FXR in huh7 cells lead to an increase in USP2. Of importance, we also found FXR directly regulates USP2 gene expression by dual luciferase assay. This study is the first to report FXR in the regulation of gene, mRNA, and protein expression of USP2 in the liver. Specifically, FXRα2 is the predominant isoform in this regulation. As previous studies have found FXR to display a protective effect in HCC, this study identifies a novel mechanism of this protection through USP2.

INTRODUCTION

Liver cancer is in the ten leading cancer types for estimated new cases and deaths in the United States in 2018, and is often detected at late stages when it is rapidly fatal (1). Risk factors include cirrhosis, hepatitis B, hepatitis C, tobacco smoking, alcohol, diabetes, and other metabolic liver disease. (2–7). Of the types of liver cancers in humans, hepatocellular carcinoma (HCC) is the most lethal and prevalent (8). An important factor in the development of HCC is Farnesoid X Receptor (FXR) (nuclear receptor subfamily 1, group H, member 4). FXR has a variety of important functions in the liver in both metabolic and non-metabolic processes. It is the master regulator of bile acid homeostasis, and plays a critical role in lipid, cholesterol, and glucose homeostasis (9–15). In addition, FXR also plays an important role in both liver regeneration and liver cancer (16–18). It has been demonstrated that the relative expression levels of two FXR isoforms, FXRα1 and FXRα2, are significantly altered in HCC (19). Furthermore, FXR has been proposed to have a protective role from hepatocarcinogenesis through its anti-inflammatory activities and ability to prevent and repair liver injury (16,20–24). However, the mechanism by which FXR signaling protects against HCC development is still unclear.

Characterization by microarray analysis of wild type and FXR-/- mice revealed multiple target genes that are regulated by FXR signaling. A large number of genes, especially those involved in cell proliferation and apoptosis, were regulated by FXR. Among these genes, Ubiquitin Specific Peptidase 2 (USP2) exhibited the most altered expression levels between wild type and FXR-/- mice. USP2 is a deubiquitinating enzyme (DUB), ultimately regulating protein stability through deubiquitination.

Posttranslational modification with ubiquitin regulates protein stability and has an essential role in regulating a variety of cellular processes. Ubiquitin can be reversed by DUBs, such as USP2, which involves hydrolysis of an isopeptide bond (25). Recent studies have shown that USP2 regulates a number of target proteins involved in cell proliferation, apoptosis, and tumorigenesis. These target proteins include cyclin A1, cyclin D1, mouse double minute 2 homolog (MDM2), MDM4, p53, fatty acid synthetase (FASN), receptor-interacting serine/threonine-protein kinase 1 (RIP1), and period circadian protein homolog 1 (PER1) (26–32). We hypothesized FXR regulates USP2 expression to protect from HCC development.

Wild type and FXR-/- mice were used for the current study. A previous study found FXR-/- mice are a useful model for HCC studies, as they resemble HCC progression in humans with altered metabolism and increased inflammatory response and fibrosis (33). We report a dysregulation for USP2a and USP2b isoforms between wild type and FXR-/- mice during both their peak and trough time points. As previous literature has shown, the USP2b isoform is a circadian gene in mice. Based upon our previous studies, we found the highest expression of USP2 mRNA to occur at 2pm, and the lowest levels to occur at 6am when lights first turn on in the morning. For this reason, these are the two time points we used for our studies. FXR-/- mice display an increase in USP2a at both time points, and a decrease in USP2b at both time points. Additionally, downstream target genes were also shown to dysregulated. MDM2 decreased slightly in FXR-/- mice, while FASN and cyclin D1 were increased compared to the wild type.

Importantly, we found that treatment of wild type mice with Obeticholic acid (OCA), a selective FXR agonist, leads to a significant increase in both USP2a and

USP2b. OCA has been found to reduce hepatic inflammation and fibrosis in a rat model of cirrhosis (34), as well as to protect against liver injury and inflammation in both lipopolysaccharide-induced (35) and carbon tetrachloride-induced liver injury (36). Notably, OCA has also been found to play a protective role in the liver. It protects against hepatocyte death and liver fibrosis in a murine model of nonalcoholic steatohepatitis (NASH) (37), and suppresses HCC proliferation and metastasis (38).

In the HCC cell line Huh7, we explored the role of co-transfection with FXRα1 and FXRα2 isoforms. When transfected with vector alone and treated with FXR agonists and antagonists, cells displayed no change in USP2 mRNA expression levels. When transfected with FXRα2 and treated with FXR agonist, USP2b expression significantly increased. Additionally, we identified two separate promoters for USP2a and USP2b. Previously, the two isoforms are suggested to be due to alternative splicing (39). However, our data suggests they in fact come from different promoters. Through a dual luciferase reporter system we found co-transfection of the USP2 promoters with FXRα2 and treated with FXR agonist leads to a dramatic increase in USP2 gene expression. This effect was not seen with transfection of the USP2 promoter alone.

Overall, FXR has been shown to play a protective role against HCC development. Activation of FXR by OCA has been shown to have a variety of protective roles in response to liver injury and against HCC. Here, we report that treatment of wild type mice with OCA leads to significant increases in USP2. Previously it has been found that USP2 is significantly reduced in human HCC tumor samples compared to normal liver samples (manuscript 1). Additionally, the current study shows FXR regulates USP2 gene expression in Huh7 cells through two promoters. Taken together, this is the

first report of USP2 displaying a protective role against HCC development via FXR regulation.

MATERIALS AND METHODS

Cell Culture: Huh7 and HepG2 liver cancer cell lines were cultured at 37ºC in a humidified atmosphere containing 5% CO_2. Fetal Bovine Serum (FBS) (Atlanta biologicals, cat #S11550) was used at 10% for passing and 1% for treatment. Dulbecco's Modified Eagle Medium (DMEM) was used for Huh7 culture and Minimum Essential Media (MEM) (Thermo Fisher Scientific, cat# 11095080) was used for HepG2. All media contained 1% PenStrep (Thermo Fisher, cat# 15140122), and 1% NEAA (Thermo Fisher, cat# 11140050).

Cell Treatments: Cells were treated with drug dissolved in dimethyl sulfoxide (DMSO) (Sigma, cat# 276855) as a vehicle. DMSO was used for control for all experiments. DY 268, a highly potent FXR antagonist, was purchased from Axon Medchem (cat# 2561) and treated at 1 μM. Chenodeoxycholic acid (CDCA) was purchased from Sigma Aldrich (cat# C9377) and was treated at 10 μM. GW4064, a selective FXR agonist, was purchased from Tocris (cat# 2473) and was treated at 1 μM.

Plasmid Constructs: Expression plasmids for human FXRα1 and FXRα2 were provided by Dr. Matthew Stoner and Dr. David Mangelsdorf (University of Texas Southwestern Medical Center).

Dual Luciferase Assay: Huh7 cells were plated at 80% confluence in 48 well plates in DMEM media. GenJet Reagent (Version II) (SignaGen, cat# SL100489) was used for transfection of USP2 promoter in luciferase vector along with co-transfection of human FXRα1 or FXRα2 into Huh7 cells according to suggested company protocol. Standard amounts of plasmid DNA was used and *Renilla* Luciferase null plasmid was used as an internal control for cell number and transfection efficiency. After transfection, cells were treated for 30 hours with FXR agonist or antagonists. Dual-Luciferase Reporter Assay System (Promega, cat# E1960) was used to determine the activity of the firefly and *Renilla* luminescence sequentially. Post treatment, cells were washed with PBS and lysis buffer was added followed by rocking. Cell lysates were transferred to a 96-well white walled plate and luciferase activities were measured using a dual injector GloMax Multimode Microplate Reader (Promega). Firefly luminescence was normalized based on *Renilla* luminescence signal, and the ratio of treatment over control served as fold activation. Data are presented as mean ± standard deviation.

Animal Experimentation General Care: All animals received humane care according to the criteria outlined in the "Guide for the Care and Use of Laboratory Animals" prepared by the National Academy of Sciences and published by the National Institutes of Health (NIH publication 86023 revised 1985). Mice were fed a regular chow diet and housed in Innovive IVC ventilated rodent housing system racks in IVC disposable cages. In total, 32 wild type mice (C57BL/6) and 17 FXR-/- mice were utilized. Of the wild type mice, 16 were female and 16 were male. Of the FXR-/- mice, 8 were female and 9 were male.

Wild Type versus FXR-/- mice samples: When comparing wild type and FXR-/- mice, the two time points previously discussed (6am and 2pm) had to be taken into consideration. All organ isolation occurred within 1 hour from these start times. For the 6am group, 5 wild type and 8 FXR-/- mice were utilized. The wild type group contained 3 females and 2 males, and the FXR-/- group contained 4 females and 4 males. For the 2pm group, 8 wild type and 9 FXR-/- mice were utilized. The wild type group contained 3 females and 5 males, and the FXR-/- group contained 4 females and 5 males. All samples were snap frozen in liquid nitrogen.

Wild Type Mice Obeticholic Acid Oral Gavage Treatment: A total of 19 wild type mice were utilized for this study. There were 8 mice in the vehicle control group, 5 of which were female and 3 were male. There were 11 mice in the treatment group, 5 of which were females and 6 were male. Their age ranged from x-x. The treatment group received a total of 5 doses of FXR agonist OCA at 50mg/kg over a course of 3 days. The control group received the vehicle, 1,2-propanediol diluted in PBS 1:4. They received 2 doses daily once in the morning and once at night for two days, and one final dose at 6am. Organ isolation started at 8am and was completed within 1 hour. All samples were snap frozen.

Quantitative real-time PCR: RNA isolation, cDNA synthesis, and TaqMan qPCR assays were performed as previously described (manuscript 1). In short, RNA was extracted from tissue and cell samples using RNA-bee according to manufacturer's

protocol (Amsbio, cat #CS-501B). M-MLV Reverse Transcriptase (Promega, cat #M170B) was utilized to synthesize cDNA. TaqMan Gene Expression Assay was utilized for analysis of cDNA. All TaqMan probes were purchased through Thermo Fisher Scientific and are as follows. Human total USP2 (cat# Hs00275859_m1), USP2a (cat# Hs00374431_m1), and USP2b (Hs01592505_m1) were purchased from catalog. Mouse total USP2 (cat# Mm00497452_m1) and USP2b (cat# Mm01168648) probes were purchased from catalog. The Custom TaqMan Assay Design Tool (cat# 4441114) was utilized for custom design of mouse USP2a probe based on NM_016808 (Assay ID ARCE37A). Applied Biosystems ViiA 7 Real-Time PCR instrument was used for quantification using the comparative C_T ($\Delta\Delta C_T$) method normalized against glyceraldehyde-3-phosphate dehydrogenase (GAPDH) housekeeper.

Western Blotting: Liver tissue was homogenized in sucrose-Tris (ST) buffer composed of 0.25 M sucrose and 10 mM Tris-HCL with ph 7.4 containing Halt Protease Inhibitor Cocktail (Thermo Scientific, cat #87785) and phenylmethylsulfonyl fluoride (PMSF) (Sigma, CAS #329986). Membrane fractions containing total proteins were loaded into each well. After overnight wet transfer to polyvinylidene difluoride (PVDF) membrane, the membrane was probed for the various USP2 isoforms. Sequence specific antibodies were purchased from Biomatik, and are detiled in supplementary table 3. Additionally, the following antibodies were purchased: Cycin D1 (Santa Cruz cat# sc-8396), FAS (Santa Cruz cat# sc-55580), MDM2 (Santa Cruz cat# sc-965), P53 (Santa Cruz, cat #sc-47698), and USP2 (Proteintech cat# 10392-1-AP). Rabbit anti-human GAPDH polyclonal antibody (Sigma-Aldrich, cat# G9545) was used as housekeepers to

normalize protein expression. Clarity and Clarity Max Western ECL Blotting Substrates (BioRad cat# 1705060) was added to membranes for chemiluminescent detection, incubated according to protocol, and imaged using myECL Imager from Thermo Scientific. ImageJ was used to quantify all bands which were normalized against GAPDH.

Statistical analysis: Student t-test was applied to pair-wise comparison for normally distributed data. Non-parametric Mann-Whitney test was used for pair-wise comparison for non-normally distributed data. P value of 0.05 or lower was considered statistically significant.

RESULTS

USP2 and downstream target genes are dysregulated between WT and FXR-/- mice.

Previous studies have found a dysregulation of the USP2 isoforms in healthy versus HCC subjections, human tumor versus surrounding samples, and murine tumor versus surrounding samples (manuscript 1). Considering FXR-/- mice resemble HCC progression in humans (33), USP2 levels were compared in wild type and FXR-/- mice. As discussed, USP2 has multiple isoforms. When looking at USP2a and USP2b in wild type versus FXR-/- mice during peak and trough time points, they have opposing relationships. During the 2pm time point, USP2a shows a significant 1.7 fold increase in expression (fig. 1a) and a 46% decrease in USP2b expression (fig. 1b) in FXR-/- mice. During the 6am time point, the USP2 isoforms follow the same trend. USP2a

shows a significant 2.6 fold increase (fig. 1c), while USP2b shows a 37% decrease (fig. 1d). Similarly, protein levels of USP2b displayed a 7% decrease in FXR-/- mice compared to wild type (fig. 2a). In addition, previous publications have shown USP2 to regulate MDM2, FASN, and cyclin D1. Compared to wild type mice, FXR-/- mice displayed a minor 16% decrease in MDM2 protein levels (fig. 2b), while FASN and cyclin D1 showed a 2 fold (fig. 2c) and 1.7 fold (fig. 2d) increase in protein levels, respectively. These results demonstrate USP2 is dysregulated between wild type and FXR-/- mice, as well as previously reported downstream USP2 protein targets. Overall, USP2b expression is decrease in FXR-/- mice while USP2a expression is increase. As FXR-/- mice mimics human HCC, the knockout of FXR leading to a decrease in USP2b expression suggests a protective role in HCC pathogenesis, and the increase in USP2a suggests a tumor formation role.

Activation of FXR in WT mice leads to increased USP2 expression.

The data comparing wild type and FXR-/- showed opposing relationships of USP2a and USP2b. To determine if activation of FXR would change expression levels of USP2, wild type mice were treated with OCA, an FXR agonist. Based upon previous studies in both humans and animals, a dose of 50mg/kg of OCA for a total of 5 doses over 3 days was chosen. FDA Full Prescribing Information for OCALIVA (obeticholic acid/OCA) animal data section doses range from 5-75mg/kg/day. The doses in clinical trials for OCA range from 10-50 mg daily for 2-72 weeks (40–43). Overall, wild type mice treated with OCA had dramatic 8.5, 3.0, and 8.5 fold increase in total USP2, USP2a, and USP2b mRNA levels, respectively (fig. 3a-c). These same samples also

showed a statistically significant increase in protein levels for both isoforms, with a 1.6 fold increase in USP2a (fig. 4a), and a 1.6 fold increase in USP2b (fig. 4b). SHP was used as a positive control to confirm FXR activation in the treatment group. As expected, SHP expression levels displayed a 2.8 fold increase following treatment (fig. 3d). Additionally, ARNTL, a main core component of the circadian clock, was probed to determine if the effects of FXR activation on USP2 is resulted from modulation of the circadian clock. As shown in fig. 3e, there were no changes ARNTL expression between vehicle and treatment, indicating that FXR signaling specifically regulates USP2 expression and FXR activation increased USP2 expression. Interestingly, both isoforms displayed increases in expression rather than opposing relationships as seen in wild type versus FXR-/- mice. Potential reasons for this effect is reviewed in the discussion.

FXR activation in HCC cells increases USP2b mRNA levels.

FXR activation in wild type mice led to increased hepatic UPS2 expression. To determine if this effect is also seen in a human cell line, Huh7 cells were transfected with pcDNA vector, FXRα1, FXRα2, or co-transfected with both isoforms. Cells were then treated with DMSO vehicle, FXR antagonist DY268, or FXR agonist GW4064. Between all transfected and treatment groups, no change in USP2a mRNA levels were seen (fig. 5a). Among all transfection groups, USP2b mRNA levels increased following GW4064 treatment. However, cells that were co-transfected with FXRα2 and FXRα1/2 saw a statistically significant 1.8 and 1.5 fold increase in USP2b following GW4064 treatment, respectively. While those transfected with pcDNA vector, FXRα1, or

FXRα1/2 only displayed a slight increase (fig. 5b). The increases in USP2b expression following GW treatment in these cells are a result from activation of endogenous FXR. These results demonstrate that FXR activation in human HCC cells increases USP2b expression, but not USP2a. In line with the OCA treatment in wild type mice, USP2b is the predominant isoform regulated by FXR.

USP2a and USP2b are transcribed from two separate promoters

Previous literature has presented USP2a and USP2b to be a result of alternative splicing of 5' exons (39). In the current study, USP2a and USP2b showed opposing relationships in wild type compared to FXR-/- mice. When wild type mice were treated with FXR agonist, a dramatic increase was seen in USP2b, while a lesser increase was seen in USP2a. Additionally, previous studies (manuscript 1) found USP2b to have tumor protective properties while USP2a had tumor promotion properties. The different characteristics of the isoforms imply a potential for two separate promoters for USP2a and USP2b. The use of multiple promoters is a complex, but frequently used, mechanism (44). Studies have shown that at least 53% of human genes have alternative promoters (45). A depiction of the promoter map is shown in fig. 6. Both USP2a and USP2c contain the same exon 1, with exon 2 removed in the USP2c isoform. USP2b does not contain exon 1 or 2 from the USP2a isoform, and has a different exon 1.

Based upon current findings of USP2a and USP2b displaying different responses, we identified the USP2a and USP2b promoters. The USP2a promoter was cloned into a luciferase reporter vector and transfected into Huh7 cells. Cells were either transfected with USP2 promoter alone, or co-transfected with FXRα1, FXRα2 or

FXRα1/2 followed by treatment with FXR agonists and antagonists. Transfection and treatment with the USP2 promoter alone showed a minimal increased in luciferase expression, likely due to endogenous expression of FXR in Huh7 cells. Co-transfection with FXRα1 showed no change among treatment groups. Co-transfection with FXRα2 showed a significant 54% decrease in luciferase when treated with FXR antagonist, and a dramatic 2.2 fold and 2.7 fold increase when treated with FXR agonists CDCA and GW4064. Co-transfection with FXRα1/2 displayed a similar trend, but overall had a less robust increase or decrease following treatment (fig. 7a).

Similar results were seen with the USP2b promoter, with no change in luciferase following promoter or FXRα1 transfection and treatment. When transfected with FXRα2 a significant 14% decrease in luciferase when treated with antagonist, and a dramatic 2.4 fold and 2.9 fold increase when treated with agonists CDCA and GW4064. This same change in USP2 expression was seen with FXRα1/2 co-transfection, but with a less robust increase (fig. 7b). To control for effects of our vector, vector was transfected with or without FXR and treated with agonist. No change in luciferase was displayed for any group besides the promoter transfected and agonist treated group (fig. 7c). Together, this data shows that the FXRα2 isoform is the predominant isoform regulating USP2 transcription.

Mapping of the FXR response elements in 1.5 kb USP2a and USP2b promoters (in progress).

After it was determined FXR regulates USP2 transcription, a series of deletions from the distal end of the 1.5kb USP2 promoters was conducted to identify the response

element. The serial deletions for USP2a include 1.0, 0.5, 0.4, 0.3, 0.2, and 0.1kb promoter reporters, and for USP2b include 1.0 and 0.5kb. All data showed the same trend of FXR activation on USP2a (fig 8a) and USP2b (fig. 8b) as the 1.5kb constructs, suggesting the FXR response element for USP2a is within the 0.1kb region, while the FXR response element for USP2b is in the 0.5kb region. To further identify the precise location of the response element, 6 element reporter constructs were cloned into a luciferase reporter vector. These results identified a potential FXRE in element 3.

DISCUSSION

A unique relationship is seen in USP2 levels between wild type and FXR-/- mice. USP2a levels are increased in FXR-/- mice while USP2b levels are decreased prior to spontaneous tumor formation seen in FXR-/- mice (8 months of age). Additionally, previously identified USP2 downstream target genes, including MDM2 (28), FASN (32), and Cyclin D1 (27), were dysregulated. MDM2 levels did not show a dramatic change between wild type and FXR-/- mice. However, FASN and Cyclin D1 displayed a 2 fold and 1.7 fold increase, respectively, in FXR-/- mice. The overexpression of FASN and Cyclin D1 have been linked to tumorigenesis in human tumors. Additionally, previous reports found USP2 to interact with and stabilize FASN in prostate cancer (32) and Cyclin D1 in 293 cells and *in vivo* (27). The first report identifies USP2a specifically, while the second report only references USP2. Based on the data in the current study, the increase seen in USP2a correlates with the increases previously seen in FASN and Cyclin D1. FXR-/- mice are used as a model of HCC progression, suggesting USP2a as a regulator of these two downstream target genes in

liver cancer. It remains to be determine whether FASN and Cyclin D are the downstream targets of USP2a, USP2b, or both.

To determine if this change in USP2 levels between wild type and FXR-/- mice was truly caused by FXR, we treated wild type mice with an FXR agonist over a course of 3 days. This activation of FXR lead to an increase in both USP2a and USP2b isoforms at the mRNA and protein level. Although previous literature has cited USP2 to be a component of the circadian clock (46–49), ARNTL, a major component of the circadian clock, was not affected by this treatment. This suggests that although USP2 is involved in circadian patterns, it can be affected by other stimuli, such as FXR activation. Interestingly, USP2a expression is increased in FXR-/- mice during both time points compared to wild type mice, while USP2b expression is decrease. However, when wild type mice were treated with an FXR agonist, both isoforms increased. USP2a increased by 3 fold and USP2b increased by 8.5 fold. The USP2b trend is what is expected considering when FXR is knocked out in mice, USP2b also decreases. This increase in USP2a, which is much less dramatic than that of USP2b, may be due to the short duration of the study. As this was a short term study only lasting a few days, the changes seen in USP2 after FXR activation can be attributed to a direct effect of this activation. For a long term study, other factors could contribute to the changes seen in USP2, such as liver damage from inflammation and degradation. USP2a was increased in the FXR-/- mice compared to wild type mice, in which both group were 8 months of age. This proposes a potential time effect of FXR activation or knockout on the USP2a isoform.

The effects of FXR were also investigated in Huh7 cells. Cells treated with transfection of FXRα1, FXRα2, or FXRα1/2 displayed no changes in USP2a

expression following FXR drug treatments. After transfection of FXRα2 and FXR activation, USP2b showed a significant increase in mRNA expression. Considering there was an increase in both USP2a and USP2b expression levels following FXR activation in mice, it was anticipated that both USP2a and USP2b would increase following FXR activation in cells. However, an increase in expression was only seen in USP2b following agonist treatment. Although no increase was seen in USP2a, this still correlates with the OCA mice treatment. A dramatic 8.5 fold increase was seen in USP2b, while only a 3.0 increase was seen in USP2a following activation in wild type mice. Considering USP2b saw the more dramatic fold increase *in vivo*, since there is only a 1.8 fold increase in expression in cells it would be expected that USP2a would show a much less fold increase. Since the increase in USP2b was so small, no increase in USP2a can be expected.

To determine if FXR regulates USP2 at the transcriptional or post-transcriptional level, USP2 promoters were characterized, and a dual luciferase promoter reporter assay was conducted using USP2a or USP2b promoters alone or co-transfected with FXRα1, FXRα2, or FXRα1/2. Activation of USP2a and USP2b promoters following FXR agonists indicated that FXR-mediated regulation of USP2a and USP2b is at the transcriptional level. A significant increase in USP2 gene expression was seen with co-transfection with FXRα2. This effect was not seen with promoter transfection alone or with FXRα1, suggesting this increase in gene expression is FXRα2 specific. Previous studies of human HCC samples comparing surrounding tissue to tumor tissue found an interesting relationship with USP2a. Of 8 paired samples, half displayed a dramatic increase in USP2a within the tumor sample, while the other half

had a dramatic decrease (manuscript 1). Interestingly, we noted that FXRα2 was either undetected or at extremely low levels in the samples with low USP2a. In line with these findings, the current study shows USP2 gene expression is primarily regulated by the FXRα2 isoform, and changes in mRNA were seen only in huh7 cells transfected with the FXRα2 isoform. No change was seen in gene expression or mRNA levels with the FXRα1 isoform alone, suggesting FXRα2 is the predominant isoform regulating USP2.

Overall, this study is the first to report FXR in the regulation of gene, mRNA, and protein expression of USP2 in the liver. Specifically, FXRα2 is the predominant isoform in this regulation. FXR plays protective roles in HCC development and is also required for liver regeneration (17,18,22,33). As reported in manuscript 1, USP2b has apoptotic activity and protects HCC development. FXR-mediated regulation of USP2b and its downstream targets may provide a mechanistic link between FXR and its protective activity on HCC development.

Supplementary Material

Refer to Web version on PubMed Central for supplementary material.

Acknowledgements

Technical and instrumental support from the RI-INBRE Core Facility in the College of Pharmacy is greatly appreciated.

References

1. Siegel RL, Miller KD, Jemal A. Cancer statistics, 2018. CA Cancer J Clin. 2018 Jan;68(1):7–30.

2. Gomaa A-I, Khan S-A, Toledano M-B, Waked I, Taylor-Robinson S-D. Hepatocellular carcinoma: epidemiology, risk factors and pathogenesis. World journal of gastroenterology : WJG. 2008;14(27):4300–8.

3. Nishioka K, Watanabe J, Furuta S, Tanaka E, Iino S, Suzuki H, et al. A high prevalence of antibody to the hepatitis C virus in patients with hepatocellular carcinoma in Japan. Cancer. 1991;67(2):429–33.

4. Bruix J, Barrera JM, Calvet X, Ercilla G, Costa J, Sanchez-Tapias JM, et al. Prevalence of antibodies to hepatitis C virus in Spanish patients with hepatocellular carcinoma and hepatic cirrhosis. Lancet. 1989;2(8670):1004–6.

5. Davila JA, Morgan RO, Shaib Y, McGlynn KA, El-Serag HB. Diabetes increases the risk of hepatocellular carcinoma in the United States: a population based case control study. Gut. 2005 Apr;54(4):533–9.

6. Bugianesi E, Leone N, Vanni E, Marchesini G, Brunello F, Carucci P, et al. Expanding the natural history of nonalcoholic steatohepatitis: From cryptogenic cirrhosis to hepatocellular carcinoma. Gastroenterology. 2002;123(1):134–40.

7. Kuper H, Tzonou A, Kaklamani E, Hsieh CC, Lagiou P, Adami HO, et al. Tobacco smoking, alcohol consumption and their interaction in the causation of hepatocellular carcinoma . International journal of cancerJournal international du cancer. 2000;85(4):498–502.

8. Balogh J, Victor D, Asham EH, Burroughs SG, Boktour M, Saharia A, et al. Hepatocellular carcinoma: a review. J Hepatocell Carcinoma. 2016 Oct 5;3:41–53.

9. Kok T, Hulzebos CV, Wolters H, Havinga R, Agellon LB, Stellaard F, et al. Enterohepatic circulation of bile salts in farnesoid X receptor-deficient mice: efficient intestinal bile salt absorption in the absence of ileal bile acid-binding protein. J Biol Chem. 2003 Oct 24;278(43):41930–7.

10. Sinal CJ, Tohkin M, Miyata M, Ward JM, Lambert G, Gonzalez FJ. Targeted disruption of the nuclear receptor FXR/BAR impairs bile acid and lipid homeostasis. Cell. 2000 Sep 15;102(6):731–44.

11. Lefebvre P, Cariou B, Lien F, Kuipers F, Staels B. Role of bile acids and bile acid receptors in metabolic regulation. Physiol Rev. 2009 Jan;89(1):147–91.

12. Modica S, Gadaleta RM, Moschetta A. Deciphering the nuclear bile acid receptor FXR paradigm. Nuclear receptor signaling. 2010;8:e005.

13. Watanabe M, Houten SM, Wang L, Moschetta A, Mangelsdorf DJ, Heyman RA, et al. Bile acids lower triglyceride levels via a pathway involving FXR, SHP, and SREBP-1c. J Clin Invest. 2004 May;113(10):1408–18.

14. Ma K, Saha PK, Chan L, Moore DD. Farnesoid X receptor is essential for normal glucose homeostasis. J Clin Invest. 2006 Apr;116(4):1102–9.

15. Zhang Y, Lee FY, Barrera G, Lee H, Vales C, Gonzalez FJ, et al. Activation of the nuclear receptor FXR improves hyperglycemia and hyperlipidemia in diabetic mice. Proc Natl Acad Sci USA. 2006 Jan 24;103(4):1006–11.

16. Huang W, Ma K, Zhang J, Qatanani M, Cuvillier J, Liu J, et al. Nuclear receptor-dependent bile acid signaling is required for normal liver regeneration. Science (New York, NY). 2006;312(5771):233–6.

17. Yang F, Huang X, Yi T, Yen Y, Moore DD, Huang W. Spontaneous development of liver tumors in the absence of the bile acid receptor farnesoid X receptor. Cancer Research. 2007;67(3):863–7.

18. Kim I, Morimura K, Shah Y, Yang Q, Ward JM, Gonzalez FJ. Spontaneous hepatocarcinogenesis in farnesoid X receptor-null mice. Carcinogenesis. 2007 May;28(5):940–6.

19. Chen Y, Song X, Valanejad L, Vasilenko A, More V, Qiu X, et al. Bile salt export pump is dysregulated with altered farnesoid X receptor isoform expression in patients with hepatocellular carcinoma. Hepatology. 2013 Apr;57(4):1530–41.

20. Geier A, Trautwein C. Bile acids are “homeotrophic” sensors of the functional hepatic capacity and regulate adaptive growth during liver regeneration. Hepatology. 2007 Jan;45(1):251–3.

21. Milona A, Owen BM, van Mil S, Dormann D, Mataki C, Boudjelal M, et al. The normal mechanisms of pregnancy-induced liver growth are not maintained in mice

lacking the bile acid sensor Fxr. Am J Physiol Gastrointest Liver Physiol. 2010 Feb;298(2):G151-158.

22. Zhang L, Wang YD, Chen WD, Wang X, Lou G, Liu N, et al. Promotion of liver regeneration/repair by farnesoid X receptor in both liver and intestine in mice. Hepatology. 2012;56(6):2336–43.

23. Jiang Y, Iakova P, Jin J, Sullivan E, Sharin V, Hong I-H, et al. Farnesoid X receptor inhibits gankyrin in mouse livers and prevents development of liver cancer. Hepatology. 2013 Mar;57(3):1098–106.

24. Hollman DAA, Milona A, van Erpecum KJ, van Mil SWC. Anti-inflammatory and metabolic actions of FXR: insights into molecular mechanisms. Biochim Biophys Acta. 2012 Nov;1821(11):1443–52.

25. Reyes-Turcu FE, Ventii KH, Wilkinson KD. Regulation and cellular roles of ubiquitin-specific deubiquitinating enzymes. Annual review of biochemistry. 2009;78:363–97.

26. Kim J, Kim W-J, Liu Z, Loda M, Freeman MR. The ubiquitin-specific protease USP2a enhances tumor progression by targeting cyclin A1 in bladder cancer. Cell Cycle. 2012 Mar 15;11(6):1123–30.

27. Shan J, Zhao W, Gu W. Suppression of Cancer Cell Growth by Promoting Cyclin D1 Degradation. Molecular Cell. 2009 Nov;36(3):469–76.

28. Stevenson LF, Sparks A, Allende-Vega N, Xirodimas DP, Lane DP, Saville MK. The deubiquitinating enzyme USP2a regulates the p53 pathway by targeting Mdm2. The EMBO Journal. 2007 Feb 21;26(4):976–86.

29. Mahul-Mellier A-L, Datler C, Pazarentzos E, Lin B, Chaisaklert W, Abuali G, et al. De-ubiquitinating proteases USP2a and USP2c cause apoptosis by stabilising RIP1. Biochimica et Biophysica Acta (BBA) - Molecular Cell Research. 2012 Aug;1823(8):1353–65.

30. Wang C-L, Wang J-Y, Liu Z-Y, Ma X-M, Wang X-W, Jin H, et al. Ubiquitin-specific protease 2a stabilizes MDM4 and facilitates the p53-mediated intrinsic apoptotic pathway in glioblastoma. Carcinogenesis. 2014 Jul;35(7):1500–9.

31. Yang Y, Duguay D, Bedard N, Rachalski a., Baquiran G, Na CH, et al. Regulation of behavioral circadian rhythms and clock protein PER1 by the deubiquitinating enzyme USP2. Biology Open. 2012;1:789–801.

32. Graner E, Tang D, Rossi S, Baron A, Migita T, Weinstein LJ, et al. The isopeptidase USP2a regulates the stability of fatty acid synthase in prostate cancer. Cancer Cell. 2004 Mar;5(3):253–61.

33. Liu N, Meng Z, Lou G, Zhou W, Wang X, Zhang Y, et al. Hepatocarcinogenesis in FXR-/- mice mimics human HCC progression that operates through HNF1α regulation of FXR expression. Molecular endocrinology. 2012;26(5):775–85.

34. Verbeke L, Mannaerts I, Schierwagen R, Govaere O, Klein S, Vander Elst I, et al. FXR agonist obeticholic acid reduces hepatic inflammation and fibrosis in a rat model of toxic cirrhosis. Sci Rep. 2016 16;6:33453.

35. Xiong X, Ren Y, Cui Y, Li R, Wang C, Zhang Y. Obeticholic acid protects mice against lipopolysaccharide-induced liver injury and inflammation. Biomed Pharmacother. 2017 Dec;96:1292–8.

36. Zhang D-G, Zhang C, Wang J-X, Wang B-W, Wang H, Zhang Z-H, et al. Obeticholic acid protects against carbon tetrachloride-induced acute liver injury and inflammation. Toxicol Appl Pharmacol. 2017 Jan 1;314:39–47.

37. Goto T, Itoh M, Suganami T, Kanai S, Shirakawa I, Sakai T, et al. Obeticholic acid protects against hepatocyte death and liver fibrosis in a murine model of nonalcoholic steatohepatitis. Sci Rep. 2018 May 25;8(1):8157.

38. Attia YM, Tawfiq RA, Ali AA, Elmazar MM. The FXR Agonist, Obeticholic Acid, Suppresses HCC Proliferation & Metastasis: Role of IL-6/STAT3 Signalling Pathway. Sci Rep. 2017 Oct 2;7(1):12502.

39. Gousseva N, Baker R. Gene structure, alternate splicing, tissue distribution, cellular localization, and developmental expression pattern of mouse deubiquitinating enzyme isoforms Usp2-45 and Usp2-69. Gene Expr. 2003;11(3–4):163–79.

40. Ali AH, Carey EJ, Lindor KD. Recent advances in the development of farnesoid X receptor agonists. Ann Transl Med [Internet]. 2015 Jan [cited 2018 Jun 1];3(1). Available from: https://www.ncbi.nlm.nih.gov/pmc/articles/PMC4293481/

41. Mudaliar S, Henry RR, Sanyal AJ, Morrow L, Marschall H-U, Kipnes M, et al. Efficacy and safety of the farnesoid X receptor agonist obeticholic acid in patients with type 2 diabetes and nonalcoholic fatty liver disease. Gastroenterology. 2013 Sep;145(3):574-582.e1.

42. Walters JRF, Johnston IM, Nolan JD, Vassie C, Pruzanski ME, Shapiro DA. The response of patients with bile acid diarrhoea to the farnesoid X receptor agonist obeticholic acid. Aliment Pharmacol Ther. 2015 Jan;41(1):54–64.

43. Neuschwander-Tetri BA, Loomba R, Sanyal AJ, Lavine JE, Van Natta ML, Abdelmalek MF, et al. Farnesoid X nuclear receptor ligand obeticholic acid for non-cirrhotic, non-alcoholic steatohepatitis (FLINT): a multicentre, randomised, placebo-controlled trial. Lancet. 2015 Mar 14;385(9972):956–65.

44. Ayoubi TA, Van De Ven WJ. Regulation of gene expression by alternative promoters. FASEB J. 1996 Mar;10(4):453–60.

45. Kimura K, Wakamatsu A, Suzuki Y, Ota T, Nishikawa T, Yamashita R, et al. Diversification of transcriptional modulation: Large-scale identification and characterization of putative alternative promoters of human genes. Genome Res. 2006 Jan;16(1):55–65.

46. Pouly D, Chenaux S, Martin V, Babis M, Koch R, Nagoshi E, et al. USP2-45 Is a Circadian Clock Output Effector Regulating Calcium Absorption at the Post-Translational Level. Oster H, editor. PLOS ONE. 2016 Jan 12;11(1):e0145155.

47. Scoma HD, Humby M, Yadav G, Zhang Q, Fogerty J, Besharse JC. The de-ubiquitinylating enzyme, USP2, is associated with the circadian clockwork and regulates its sensitivity to light. PLoS ONE. 2011;6(9):e25382.

48. Tong X, Buelow K, Guha A, Rausch R, Yin L. USP2a Protein Deubiquitinates and Stabilizes the Circadian Protein CRY1 in Response to Inflammatory Signals. Journal of Biological Chemistry. 2012 Jul 20;287(30):25280–91.

49. Yang Y, Duguay D, Fahrenkrug J, Cermakian N, Wing SS. USP2 Regulates the Intracellular Localization of PER1 and Circadian Gene Expression. Journal of Biological Rhythms. 2014 Aug;29(4):243–56.

Fig. 1

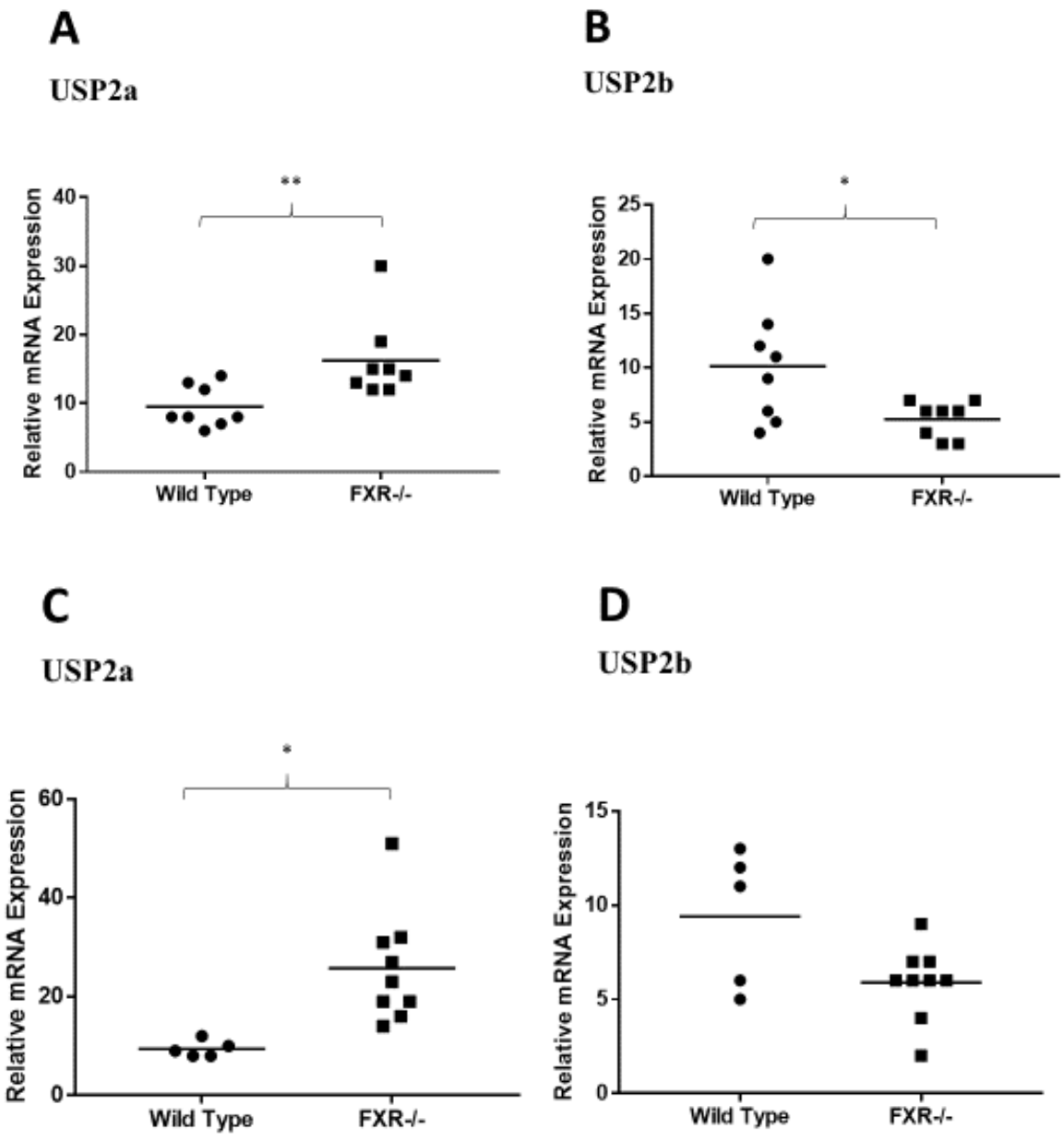
A
USP2a
**
Relative mRNA Expression
40
30
20
10
0
Wild Type
FXR-/-
B
USP2b
*
Relative mRNA Expression
25
20
15
10
5
0
Wild Type
FXR-/-
C
USP2a
*
Relative mRNA Expression
60
40
20
0
Wild Type
FXR-/-
D
USP2b
Relative mRNA Expression
15
10
5
0
Wild Type
FXR-/-

Fig. 2 A

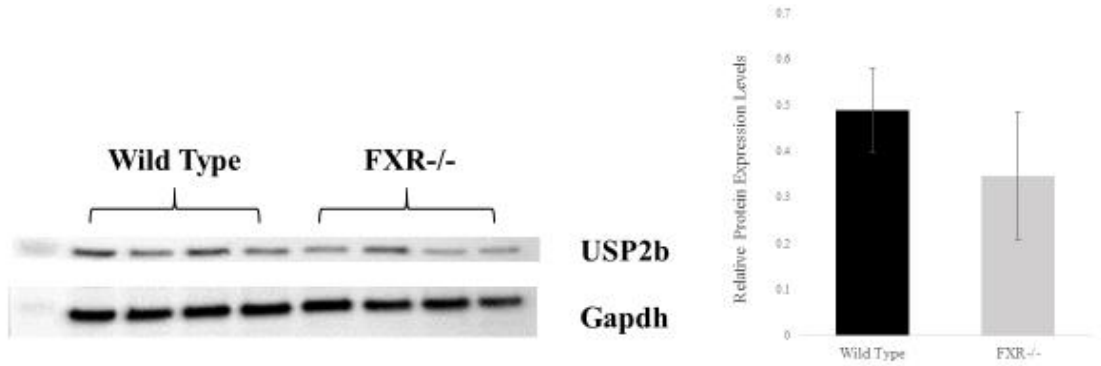
Wild Type
FXR-/-
USP2b
Gapdh
Relative Protein Expression Levels
0.7
0.6
0.5
0.4
0.3
0.2
0.1
0
Wild Type
FXR-/-

Fig. 2 B

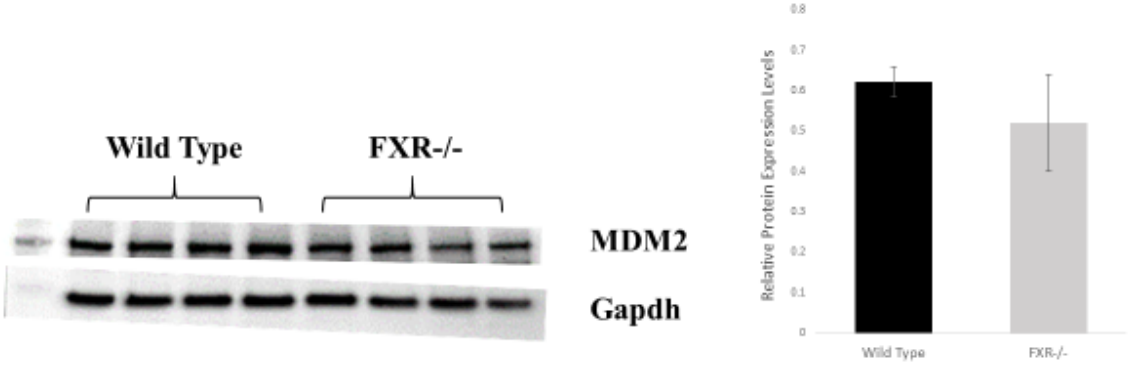
Wild Type
FXR-/-
MDM2
Gapdh
Relative Protein Expression Levels
0.8
0.7
0.6
0.5
0.4
0.3
0.2
0.1
0
Wild Type
FXR-/-

Fig. 2 C

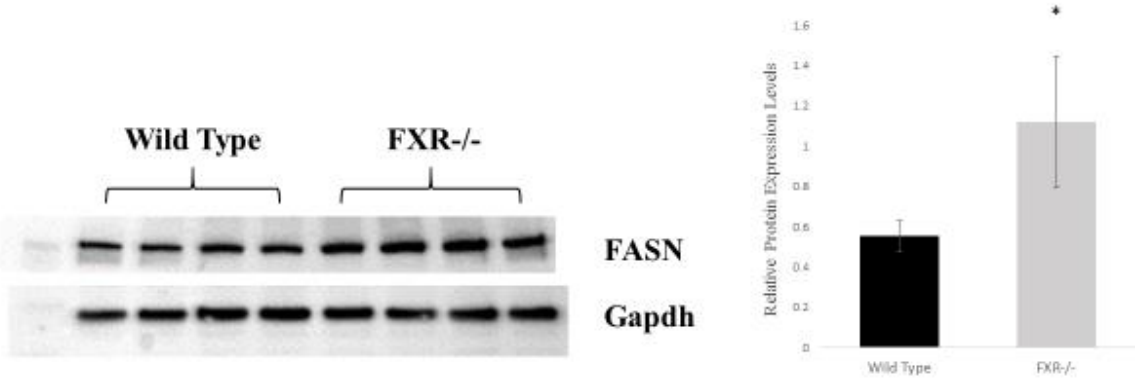
Wild Type
FXR-/-
FASN
Gapdh
Relative Protein Expression Levels
1.6
1.4
1.2
1
0.8
0.6
0.4
0.2
0
*
Wild Type
FXR-/-

Fig. 2 D

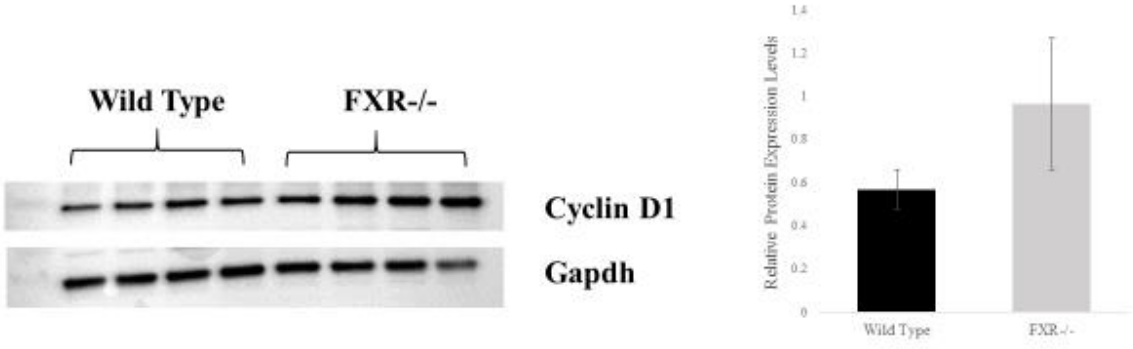
Wild Type
FXR-/-
Cyclin D1
Gapdh
Relative Protein Expression Levels
1.4
1.2
1
0.8
0.6
0.4
0.2
0
Wild Type
FXR-/-

Fig. 3

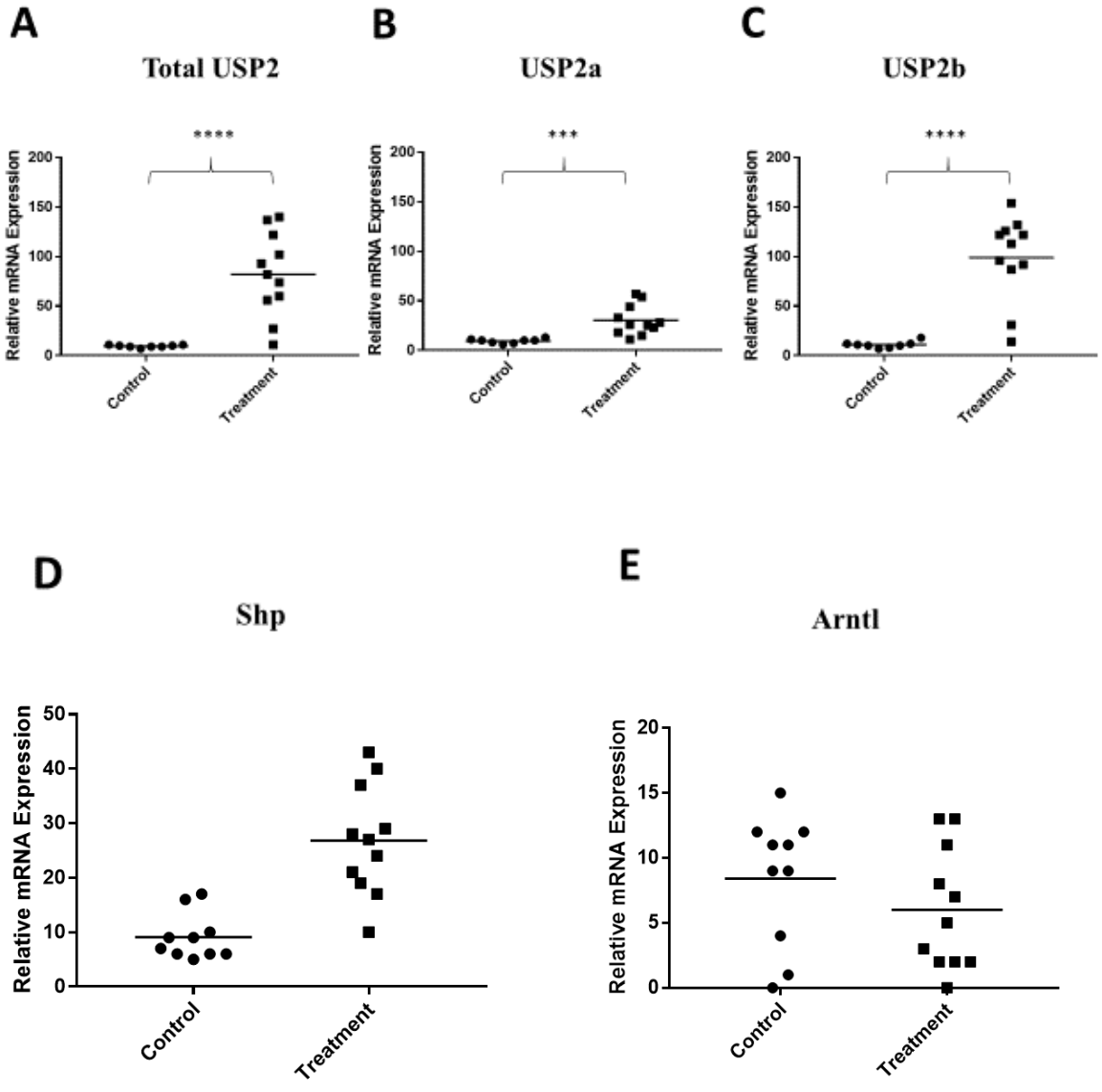
A
Total USP2
****
Relative mRNA Expression
200
150
100
50
0
Control
Treatment
B
USP2a
***
Relative mRNA Expression
200
150
100
50
0
Control
Treatment
C
USP2b
****
Relative mRNA Expression
200
150
100
50
0
Control
Treatment
D
Shp
Relative mRNA Expression
50
40
30
20
10
0
Control
Treatment
E
Arntl
Relative mRNA Expression
20
15
10
5
0
Control
Treatment

Fig. 4 A

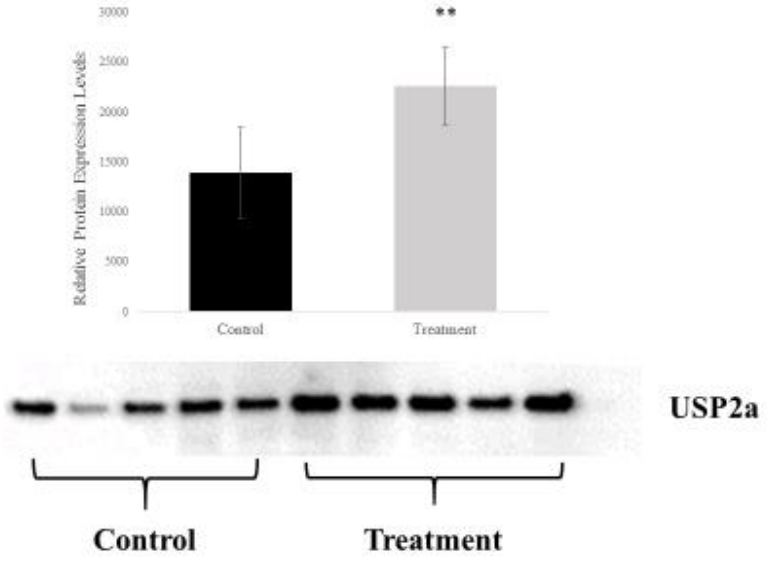
**
Relative Protein Expression Levels
30000
25000
20000
15000
10000
5000
0
Control
Treatment
USP2a
Control
Treatment

Fig. 4 B

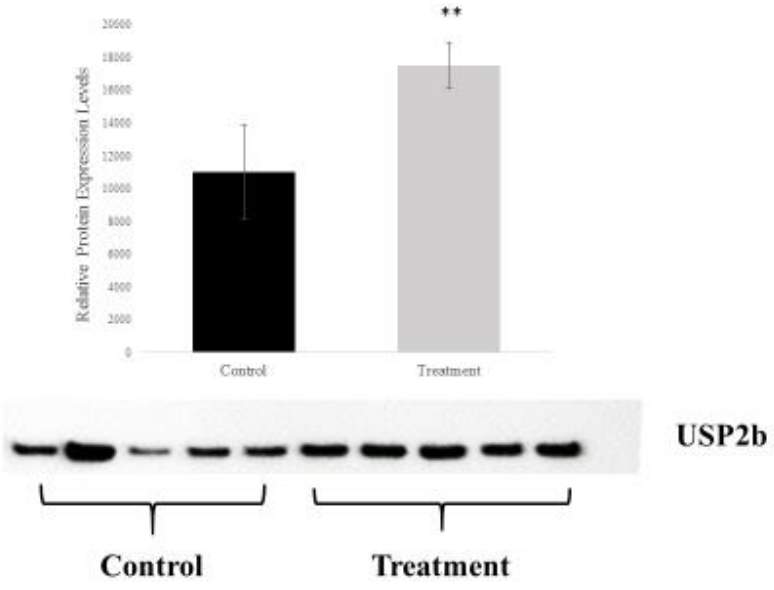
**
Relative Protein Expression Levels
20000
18000
16000
14000
12000
10000
8000
6000
4000
2000
0
Control
Treatment
USP2b
Control
Treatment

Fig. 5 A

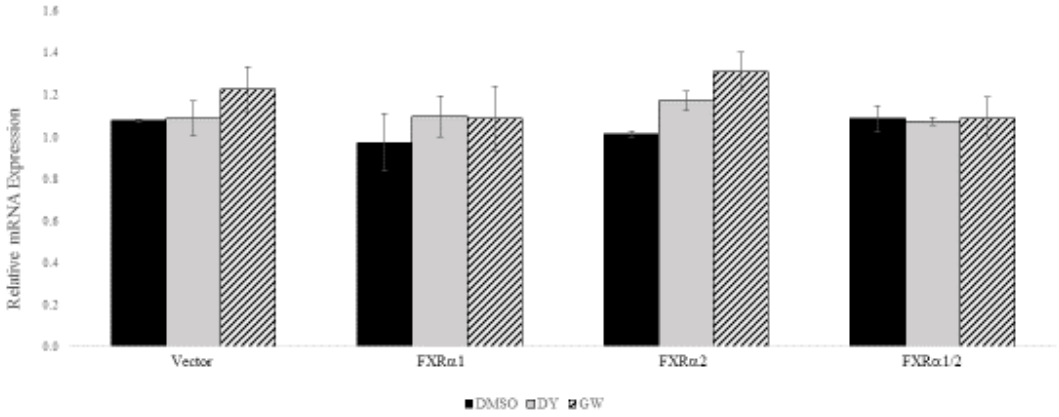
Relative mRNA Expression
1.6
1.4
1.2
1.0
0.8
0.6
0.4
0.2
0.0
Vector
FXRα1
FXRα2
FXRα1/2
DMSO
DY
GW

Fig. 5 B

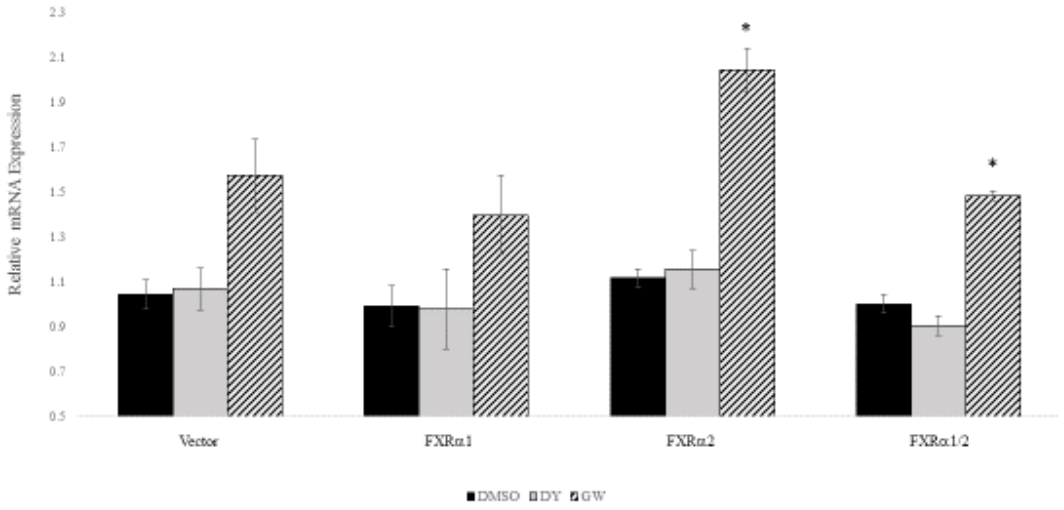
Relative mRNA Expression
2.3
2.1
1.9
1.7
1.5
1.3
1.1
0.9
0.7
0.5
*
*
Vector
FXRα1
FXRα2
FXRα1/2
DMSO
DY
GW

Fig. 6

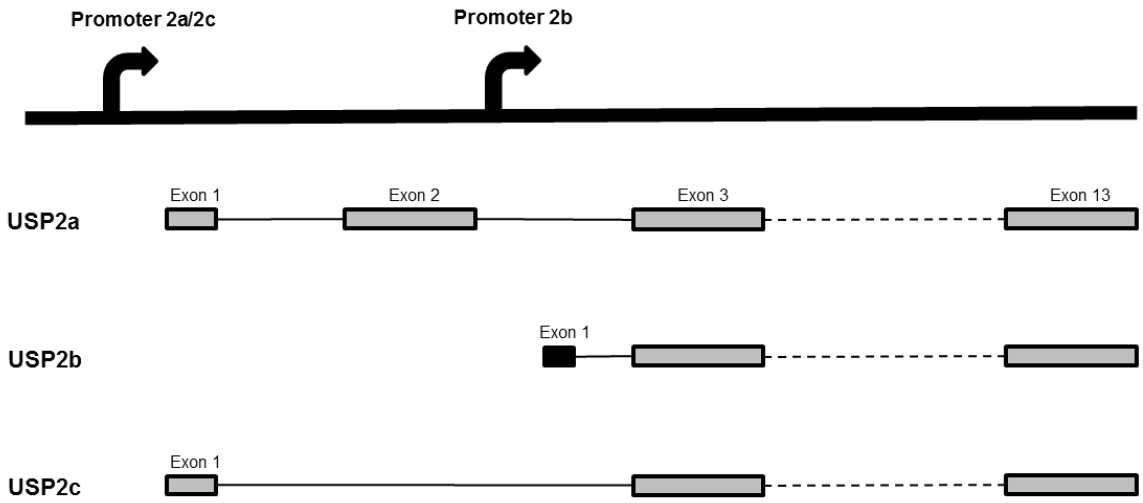
Promoter 2a/2c
Promoter 2b
USP2a
Exon 1
Exon 2
Exon 3
Exon 13
USP2b
Exon 1
USP2c
Exon 1

Fig. 7 A

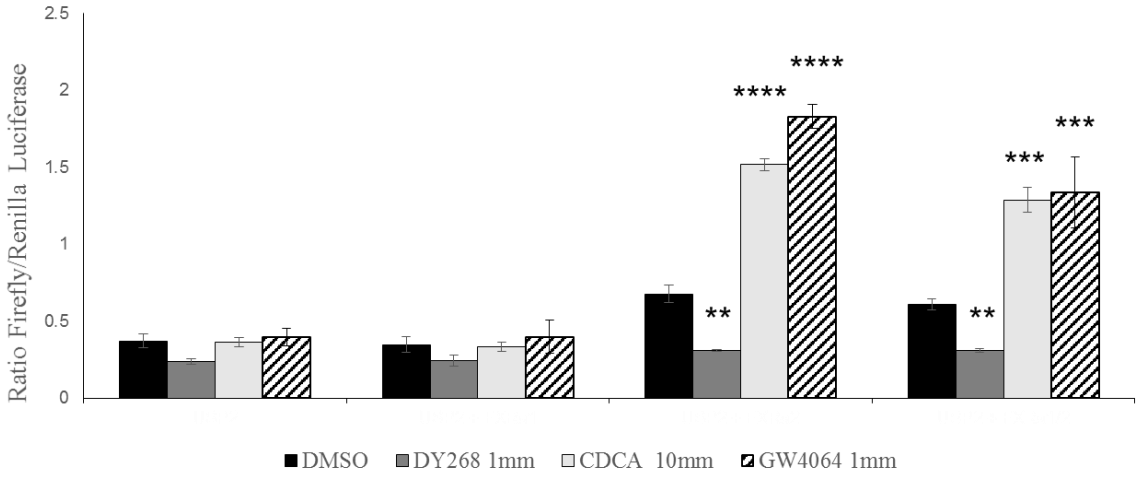
Ratio Firefly/Renilla Luciferase
2.5
2
1.5
1
0.5
0
****
****
***
***
**
**
DMSO
DY268 1mm
CDCA 10mm
GW4064 1mm

Fig. 7 B

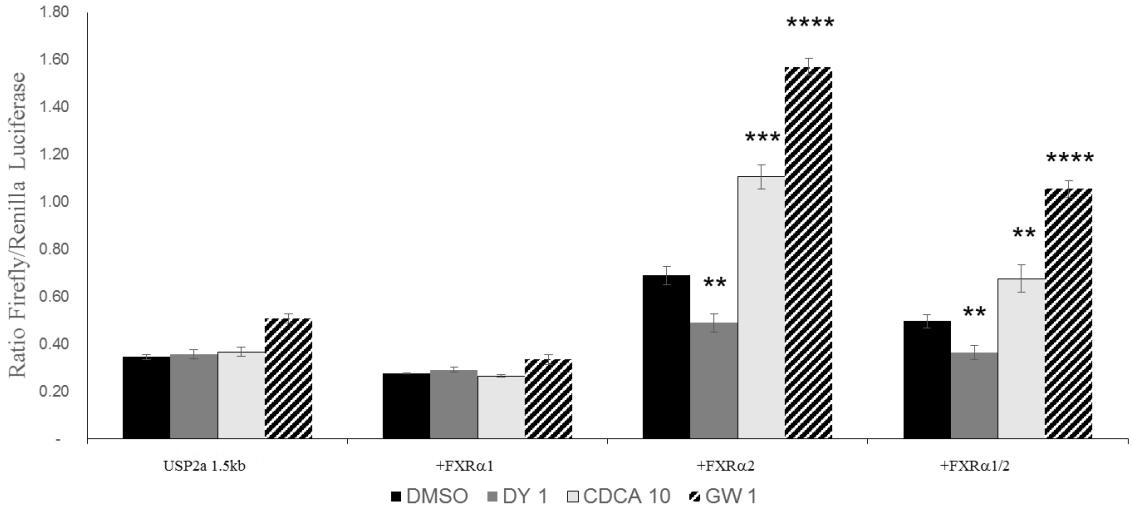
Ratio Firefly/Renilla Luciferase
1.80
1.60
1.40
1.20
1.00
0.80
0.60
0.40
0.20
-
**
***
****
**
**
****
USP2a 1.5kb
+FXRα1
+FXRα2
+FXRα1/2
DMSO
DY 1
CDCA 10
GW 1

Fig. 7 C

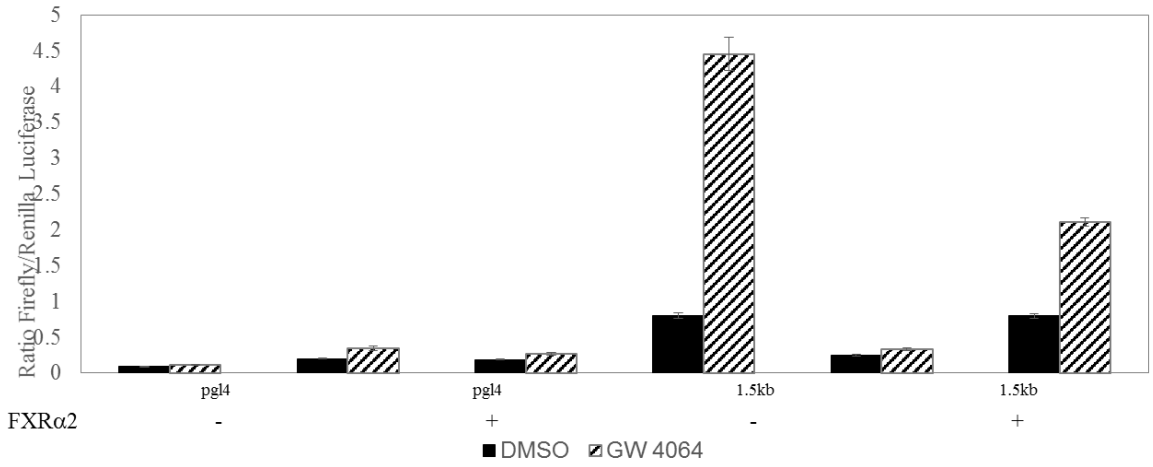
Ratio Firefly/Renilla Luciferase
5
4.5
4
3.5
3
2.5
2
1.5
1
0.5
0
pgl4
pgl4
1.5kb
1.5kb
FXRα2
-
+
-
+
DMSO
GW 4064

Fig. 8 A

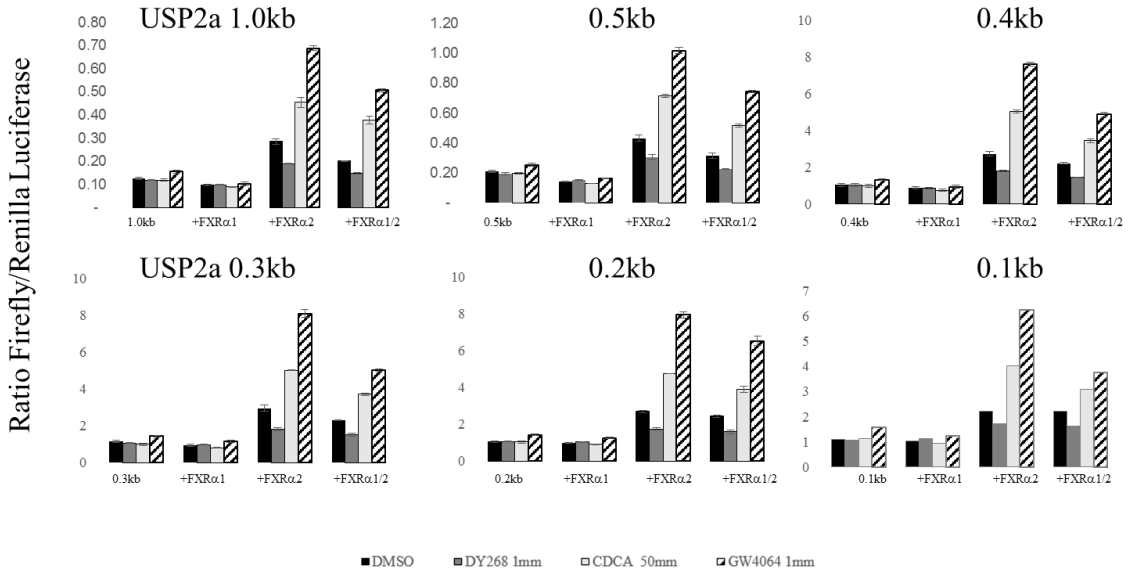
USP2a 1.0kb
0.5kb
0.4kb
USP2a 0.3kb
0.2kb
0.1kb
Ratio Firefly/Renilla Luciferase
1.0kb
0.5kb
0.4kb
0.3kb
0.2kb
0.1kb
+FXRα1
+FXRα2
+FXRα1/2
DMSO
DY268 1mm
CDCA 50mm
GW4064 1mm

Fig. 8 B

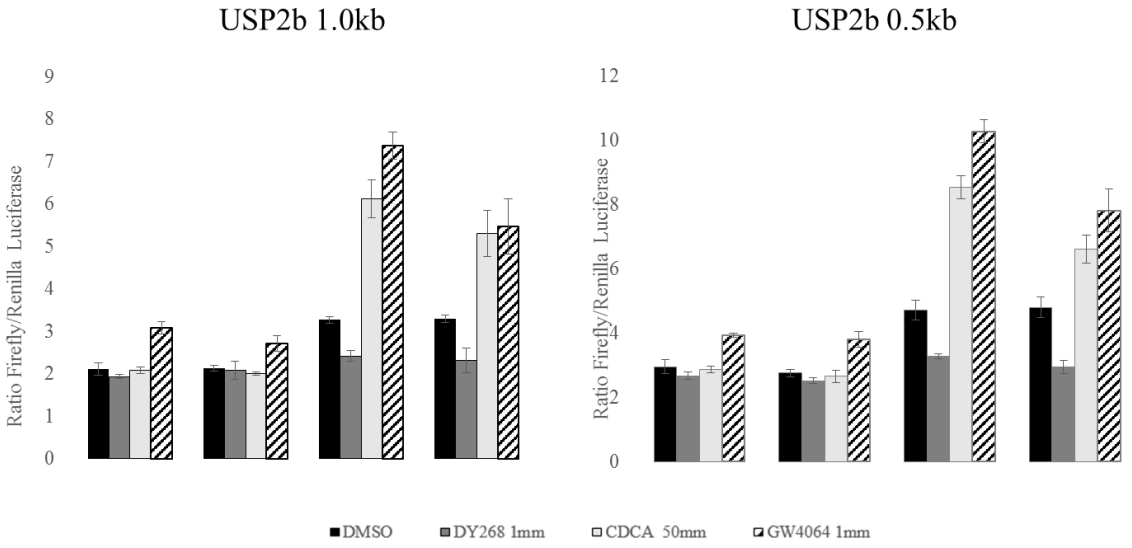
USP2b 1.0kb
USP2b 0.5kb
Ratio Firefly/Renilla Luciferase
DMSO
DY268 1mm
CDCA 50mm
GW4064 1mm

FIGURE LEGENDS

Fig. 1. USP2 mRNA levels are dysregulated between Wild Type and FXR-/- Mice at peak and trough time point in the liver. Wild type and FXR-/- liver were compared at the highest (2:00pm) and lowest levels of USP2 mRNA expression (6:00am). A single asterisk (*) indicates $p<0.05$ and a double asterisk (**) indicates $p<0.01$. (A) A significant increase in mRNA levels of USP2a was seen in FXR-/- mice compared to wild type, (B) while a significant decrease in mRNA levels of USP2b was seen at the 2pm time point. Similarly, this same trend was seen at the 6am time point with a (C) significant increase in USP2a expression in FXR-/- mice, and a (D) decrease in USP2b.

Fig. 2. USP2 and downstream target protein levels are dysregulated between Wild Type and FXR-/- Mice. Wild type and FXR-/- liver samples were compared to analyze USP2 and downstream target protein expression. A single asterisk (*) indicates $p<0.05$. (A) Consistent with mRNA expression, protein levels of USP2b are decreased within FXR-/- mice. Additionally, downstream target genes are also affected. (B) MDM2 protein levels are slightly decrease in FXR-/- mice, while (C) FASN and (D) Cyclin D1 display increased expression.

Fig. 3. Treatment with FXR agonist OCA increases USP2 mRNA expression in the liver. Wild type mice were treated with OCA at 50mg/kg for a total of 5 doses over a course of 3 days. A single asterisk (*) indicates $p<0.05$, double asterisk (**) indicates $p<0.01$, triple asterisk (***) indicates $p<0.001$, and a quadruple asterisks (****)

indicates $p<0.0001$. (A) Total USP2 (B) USP2a, and (C) USP2b mRNA levels were all significantly increased in the treatment group compared to vehicle control. (D) SHP was used as a positive control to ensure FXR activation following treatment. (E) No change was seen in ARNTL, a core component of the circadian clock.

Fig. 4. Treatment with FXR agonist OCA increases USP2 protein expression in the liver. Wild type mice were treated with OCA at 50mg/kg for a total of 5 doses over a course of 3 days. A double asterisk (**) indicates $p<0.01$. Both (A) USP2a and (B) USP2b displayed significant increases in protein levels following treatment.

Fig. 5. USP2B mRNA increases after transfection and activation of FXR. Huh7 cells were transfected with vector, FXRα1, FXRα2, or co-transfected with both isoforms, and treated with FXR antagonist DY 268 or agonist GW 4064. A single asterisk (*) indicates $p<0.05$. (A) No change in USP2a mRNA expression levels was seen for any isoform transfection or treatment. (B) USP2b mRNA levels were significantly increased in the FXRα2 and FXRα1/2 groups following FXR activation.

Fig 6. USP2a and USP2b are transcribed from two separate promoters. Based upon the current study and previous studies, the expression levels and responses seen between USP2a and USP2b are very different. The different characteristics of the isoforms imply a potential for two separate promoters for USP2a and USP2b. Here, a map of the two promoter regions is depicted.

Fig. 7. FXR Regulates the USP2a and USP2b Promoter. Huh7 cells were transfected with (A) USP2a or (B) USP2b promoter either alone or co-transfected with FXRα1, FXRα2, or FXRα1/2, followed by treatment with FXR antagonist DY 268 or agonists CDCA and GW 4064. A single asterisk (*) indicates $p<0.05$, double asterisk (**) indicates $p<0.01$, triple asterisk (***) indicates $p<0.001$, and a quadruple asterisk (****) indicates $p<0.0001$. (A) Following transfection with the USP2a promoter, no increase is seen in gene expression with transfection of the promoter alone or with FXRα1. Co-transfection with FXRα2 and treatment with FXR agonists lead to a significant increase in USP2 gene expression, while antagonism lead to a significant decrease. Co-transfection with FXRα1/2 and treatment with FXR agonists lead to a significant increase in USP2 gene expression, while antagonism lead to a significant decrease, However, changes were stunted compared to FXRα2 co-transfection. (B) Similar results were seen with the USP2b promoter. (C) Additionally, pGL3 luciferase vector had no effect on USP2. Huh7 cells were transfected with empty luciferase vector or USP2 promoter with or without FXRα2 and treated with FXR agonist GW4064. The only increase in luciferase ratio was seen in the USP2 promoter co-transfected with FXRα2, determining this increase in luciferase is indeed dependent on FXRα2 co-transfection, and not from the vector or treatment alone.

Fig. 8. Mapping of the FXR response elements in 1.5 kb USP2a and USP2b promoters (in progress). After it was determined FXR regulates USP2 transcription, a series of deletions from the distal end of the 1.5kb USP2 promoters was conducted to identify the response element. The serial deletions for (A) USP2a include 1.0, 0.5, 0.4,

0.3, 0.2, and 0.1kb promoter reporters, and for (B) USP2b include 1.0 and 0.5kb. All data showed the same trend of FXR activation on (A) USP2a and (B) USP2b as the 1.5kb constructs, suggesting the FXR response element for USP2a is within the 0.1kb region, while the FXR response element for USP2b is in the 0.5kb region.

APPENDIX

Hepatocellular carcinoma (HCC) is one of the leading causes of cancer related deaths in the United States. HCC has a 5 year survival rate of only ~15% for all stages and ~3% for distant stages (1). Unfortunately, it is often detected at late stages when it is rapidly fatal. Risk factors include cirrhosis, hepatitis B, hepatitis C, tobacco smoking, alcohol, diabetes, and other metabolic liver disease. (2–7). Of interest in HCC is farnesoid X receptor (FXR), the nuclear receptor through which bile acids exert their functions through. FXR maintains bile acid homeostasis by regulating CYP7A1 and CYP8B1, which convert cholesterol into bile acids, hepatic export transporters such as bile salt export pump (BSEP) and ABCB4, which transports bile acids out of the liver and into the bile, and hepatic uptake transporters such as NTCP and OATPs. In addition, FXR has a wide range of functions beyond regulation of bile acids, including protective effects from HCC, liver regeneration, and anti-inflammatory activity (8–11). Elevated intrahepatic bile acids due to FXR knockout can lead to cholestatic liver injury in the short term, and HCC in the long term (12). Of importance, mice FXR KO models resemble HCC progression in humans. They display altered metabolism, elevated inflammation response, and fibrosis (13). It has also been reported that FXR knockout mice spontaneously develop HCC as they age (10). Although FXR has been implicated in protection against HCC, the mechanism by which it exerts its protective effects are unclear.

Preliminary studies have been conducted using wild type and FXR knock out mice. Characterization by microarray analysis revealed ubiquitin specific peptidase 2 (USP2) as a gene of interest. USP2 is a deubiquitinating (DUB) enzyme, ultimately

regulating protein stability through deubiquitination. Posttranslational modification with ubiquitin regulates protein stability and has an essential role in regulating a variety of cellular processes. Ubiquitin can be reversed by DUB, such as USP2, which involves hydrolysis of an isopeptide bond (14). Recent studies have shown that USP2 regulates a number of target proteins involved in cell proliferation, apoptosis, and tumorigenesis. These target proteins include cyclin D1 (15), cyclin A1 (16), mouse double minute 2 homolog (MDM2) (17), receptor-interacting serine/threonine-protein kinase 1 (RIP1) (18), and period circadian protein homolog 1 (PER1) (19).

Based upon the identified trends and an abundance of literature implicating USP2 in tumorigenesis, we explore the role of the various USP2 isoforms in HCC. Additionally, we investigate how FXR regulates USP2, as well as the identification of two separate promoters.

Methods, instrumentation, and techniques are thoroughly described in the manuscripts. In summary, Huh7 and HepG2 immortalized cell lines were used for cell based assays and for treatment with FXR agonists or antagonist drugs. GenJet Reagent (Version II) was used for transfection of USP2 and FXR plasmid constructs. Cell based assays include colony formation, proliferation, apoptosis and necrosis, wound healing, migration, and invasion. Human liver samples included healthy subjects, HCC paired tumor and surrounding tissue, and HCC tumor tissue. Wild type and FXR-/- mice were utilized for FXR activation studies and tumor studies. Total RNA was prepared by phenol-chloroform extraction and used to synthesize cDNA for TaqMan qPCR analysis. Applied Biosystems ViiA 7 Real-Time PCR instrument was used for quantification using the comparative C_T ($\Delta\Delta C_T$) method. Western blot was used for protein analysis

and was imaged using myECL Imager from Thermo Scientific. Dual Luciferase Reporter Assay system was used to measure gene expression using a dual injector GloMax Multimode Microplate Reader.

Based upon the findings of the two manuscripts, USP2 is a very promising area for cancer research, specifically HCC. Consistently, USP2b is decreased within HCC subjects and in tumor mouse models. In addition, it is clear that there is a significant relationship between USP2 and FXR. This study is the first to report FXR regulating USP2 at the transcriptional level, specifically FXRα2. A previous publication by the Deng lab has also shown FXRα2 diminishes significantly, or is even untraceable, in HCC tumor samples (20). Based upon the current and previous findings, regulation of USP2 by FXR in HCC is a promising avenue to explore.

References

1. Siegel RL, Miller KD, Jemal A. Cancer statistics, 2016. CA: a cancer journal for clinicians. 2016;00(0):1–20.

2. Gomaa A-I, Khan S-A, Toledano M-B, Waked I, Taylor-Robinson S-D. Hepatocellular carcinoma: epidemiology, risk factors and pathogenesis. World journal of gastroenterology : WJG. 2008;14(27):4300–8.

3. Nishioka K, Watanabe J, Furuta S, Tanaka E, Iino S, Suzuki H, et al. A high prevalence of antibody to the hepatitis C virus in patients with hepatocellular carcinoma in Japan. Cancer. 1991;67(2):429–33.

4. Bruix J, Barrera JM, Calvet X, Ercilla G, Costa J, Sanchez-Tapias JM, et al. Prevalence of antibodies to hepatitis C virus in Spanish patients with hepatocellular carcinoma and hepatic cirrhosis. Lancet. 1989;2(8670):1004–6.

5. JA D, RO M, Y S, KA M, HB ES. Diabetes increases the risk of hepatocellular carcinoma in the United States: a population based case control study. Gut. 2005;54(4):533–9.

6. Bugianesi E, Leone N, Vanni E, Marchesini G, Brunello F, Carucci P, et al. Expanding the natural history of nonalcoholic steatohepatitis: From cryptogenic cirrhosis to hepatocellular carcinoma. Gastroenterology. 2002;123(1):134–40.

7. Kuper H, Tzonou A, Kaklamani E, Hsieh CC, Lagiou P, Adami HO, et al. Tobacco smoking, alcohol consumption and their interaction in the causation of hepatocellular carcinoma . International journal of cancerJournal international du cancer. 2000;85(4):498–502.

8. Zhang L, Wang YD, Chen WD, Wang X, Lou G, Liu N, et al. Promotion of liver regeneration/repair by farnesoid X receptor in both liver and intestine in mice. Hepatology. 2012;56(6):2336–43.

9. Huang W, Ma K, Zhang J, Qatanani M, Cuvillier J, Liu J, et al. Nuclear receptor-dependent bile acid signaling is required for normal liver regeneration. Science (New York, NY). 2006;312(5771):233–6.

10. Yang F, Huang X, Yi T, Yen Y, Moore DD, Huang W. Spontaneous development of liver tumors in the absence of the bile acid receptor farnesoid X receptor. Cancer Research. 2007;67(3):863–7.

11. Modica S, Gadaleta RM, Moschetta A. Deciphering the nuclear bile acid receptor FXR paradigm. Nuclear receptor signaling. 2010;8:e005.

12. Halilbasic E, Claudel T, Trauner M. Bile acid transporters and regulatory nuclear receptors in the liver and beyond. Vol. 58, Journal of Hepatology. 2013. p. 155–68.

13. Liu N, Meng Z, Lou G, Zhou W, Wang X, Zhang Y, et al. Hepatocarcinogenesis in FXR-/- mice mimics human HCC progression that operates through HNF1α regulation of FXR expression. Molecular endocrinology. 2012;26(5):775–85.

14. Reyes-Turcu FE, Ventii KH, Wilkinson KD. Regulation and cellular roles of ubiquitin-specific deubiquitinating enzymes. Annual review of biochemistry. 2009;78:363–97.

15. Shan J, Zhao W, Gu W. Suppression of Cancer Cell Growth by Promoting Cyclin D1 Degradation. Molecular Cell. 2009 Nov;36(3):469–76.

16. Kim J, Kim W-J, Liu Z, Loda M, Freeman MR. The ubiquitin-specific protease USP2a enhances tumor progression by targeting cyclin A1 in bladder cancer. Cell Cycle. 2012 Mar 15;11(6):1123–30.

17. Stevenson LF, Sparks A, Allende-Vega N, Xirodimas DP, Lane DP, Saville MK. The deubiquitinating enzyme USP2a regulates the p53 pathway by targeting Mdm2. The EMBO Journal. 2007 Feb 21;26(4):976–86.

18. Mahul-Mellier A-L, Datler C, Pazarentzos E, Lin B, Chaisaklert W, Abuali G, et al. De-ubiquitinating proteases USP2a and USP2c cause apoptosis by stabilising RIP1. Biochimica et Biophysica Acta (BBA) - Molecular Cell Research. 2012 Aug;1823(8):1353–65.

19. Yang Y, Duguay D, Fahrenkrug J, Cermakian N, Wing SS. USP2 Regulates the Intracellular Localization of PER1 and Circadian Gene Expression. Journal of Biological Rhythms. 2014 Aug;29(4):243–56.

20. Chen Y, Song X, Valanejad L, Vasilenko A, More V, Qiu X, et al. Bile salt export pump is dysregulated with altered farnesoid X receptor isoform expression in patients with hepatocellular carcinoma. Hepatology. 2013 Apr;57(4):1530–41.